Rational Catalyst Design for Enhanced and Controlled Growth of CNT Carpets via Water-Assisted CVD

Placidus Amama[1,2]

[1]AFRL/RXAN, WP-AFB, Ohio, USA

[2]University of Dayton Research Institute,

University of Dayton

Ohio, USA

Integrity ★ Service ★ Excellence

THE AIR FORCE RESEARCH LABORATORY

LEAD | DISCOVER | DEVELOP | DELIVER

Acknowledgements

Funding

JSPS Japan Society for the Promotion of Science

JSPS Fellowship (Nov 9, 2012 to Jan 7, 2013)

Hosts

Prof. Shigeo Maruyama
Dept. of Mechanical Eng.
The University of Tokyo

- **Prof. Shohei Chiashi**
- **Maiko Terao**

Prof. Suguru Noda
Dept. of Applied Chemistry
Waseda University

DISTRIBUTION A. Approved for public release; distribution unlimited.

Outline

- Motivation and overview
- Role of water and growth termination
  - *Ostwald ripening & subsurface diffusion phenomena*
- Influence of support-metal interactions (SMI)
  - *Carpet growth (catalyst activity & lifetime)*
  - *3D evolution of the catalyst*
- Features of a good catalyst support
  - *Porosity*
  - *Active site density*
  - *Powerful tool for predicting activity of supports*
- Conclusions

Vertically Aligned SWCNTs

- "Carpets" or "forests" of SWCNTs are of interest in a number of applications
  - Membranes
  - Supercapacitors
  - Super hydrophobic surfaces
  - "Gecko" tapes
  - Li ion batteries
  - Polymer-nanotube composites
  - Field emission sources
- Collective properties and carpet / SWCNT uniformity are important

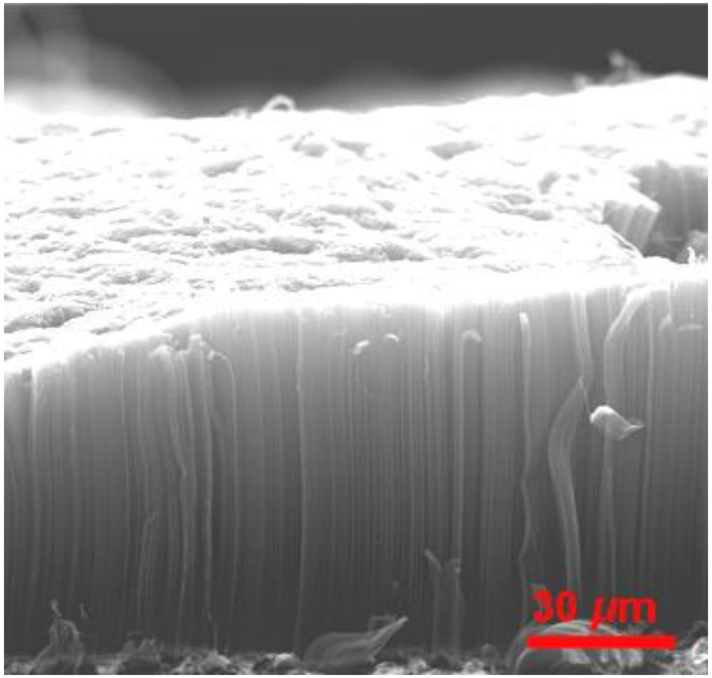

Growing Carbon Nanotubes

- **Inputs**
  - Energy (heat)
  - Very small metal catalyst
  - Carbon source
- **Typical Growth Processes**
  - Carbon arc discharge
  - Laser ablation
  - Chemical vapor deposition (CVD)
    - *Thermal CVD*
      - HiPco
      - Hydrocarbon
    - *Plasma-enhanced CVD*
      - Microwave
      - DC
      - Rf

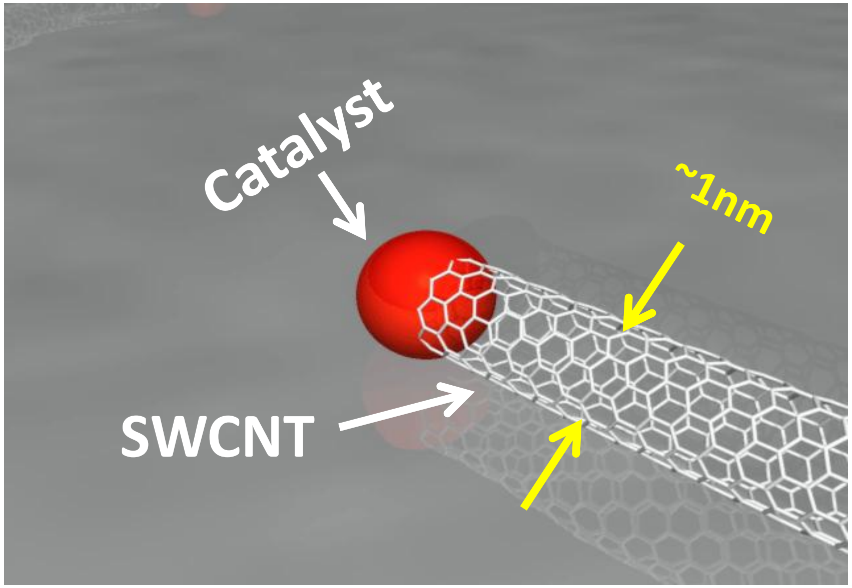

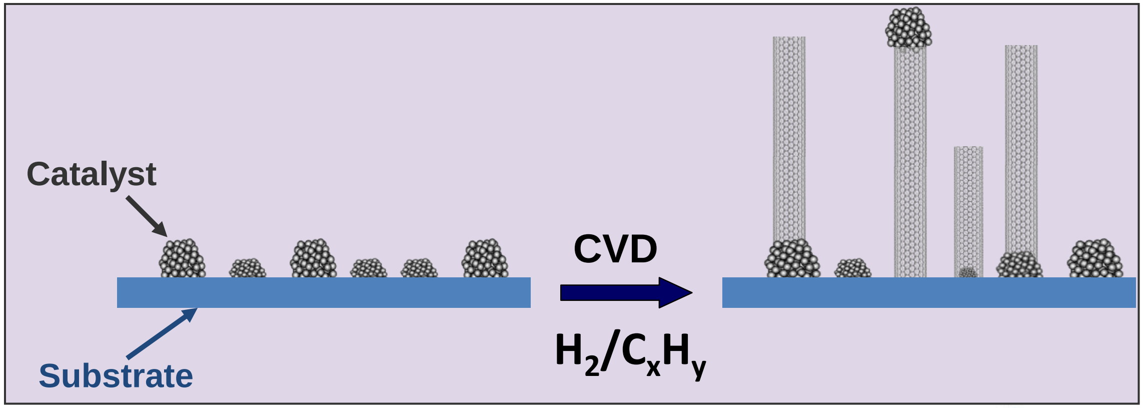

Vertically Aligned SWCNT Growth

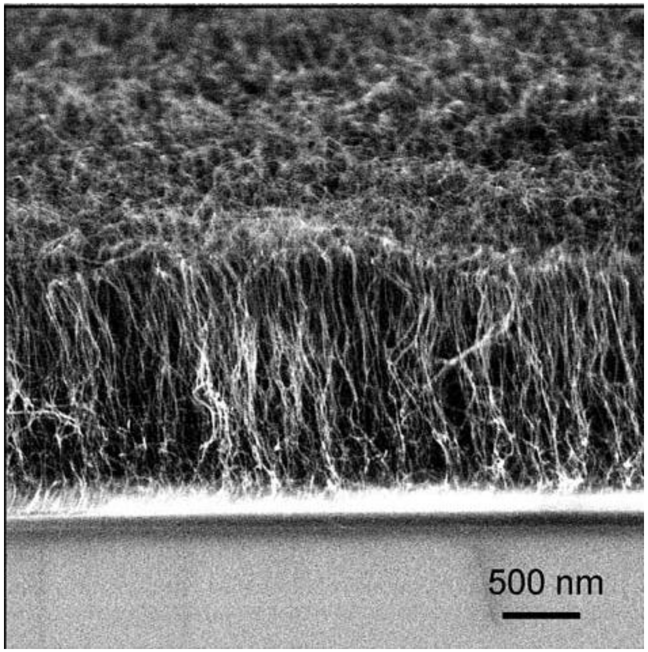

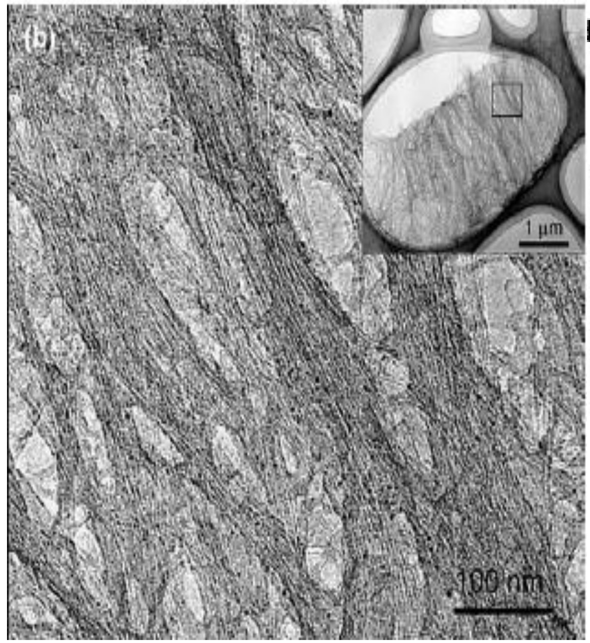

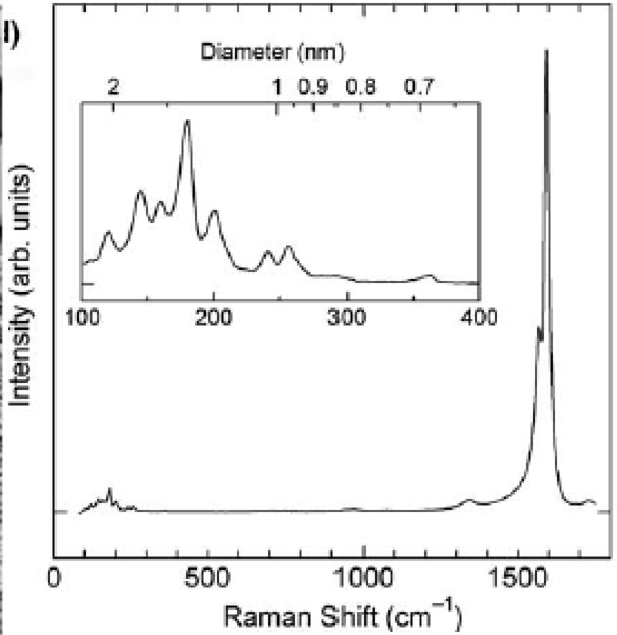

- First report of SWCNT carpet growth was performed using alcohol CVD at 800°C on quartz-supported Co-Mo catalyst
  - Growth for 1h leads to 1.5 µm long tubes
  - SWCNT growth requires high temperatures, leading to catalyst 'poisoning'

Murakami et al., *Chem. Phys. Lett.*, **2004**, *385*, 298.

Water-Assisted Growth or 'Supergrowth' of SWCNT Carpet

- Activity and lifetime of the catalysts are enhanced by water
- Highly dense SWCNT carpets up to 2.5 mm are grown
- Carbon purity of carpets is >99.98%
- But growth terminates after about 20 – 30 min

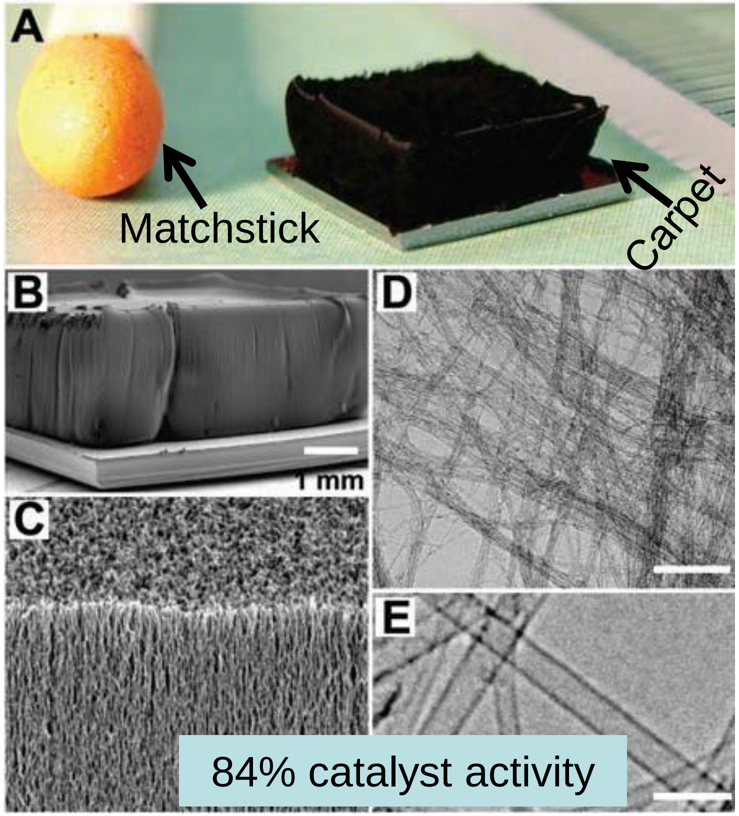

What is the role of water during super growth?

(1) K. Hata, D.N. Futaba, K. Mizuno, T. Namai, M. Yumura, S. Iijima, *Science* **2004**, *306*, 1362
(2) Futaba, Hata, Namai, Yamada, Mizuno, Hayamizu, Yumura, Iijima,., *J. Phys. Chem. B* **2006**, *110*, 8035
(3) Futaba, Hata, Yamada, Mizuno, Yumura, Iijima, *Phys. Rev. Lett.* **2005**, *95*, 056104

Outline

- Motivation and overview
- Role of water and growth termination
  - *Ostwald ripening & subsurface diffusion phenomena*
- Influence of support-metal interactions (SMI)
  - *Carpet growth (catalyst activity & lifetime)*
  - *3D evolution of the catalyst*
- Features of a good catalyst support
  - *Porosity*
  - *Active site density*
  - *Powerful tool for predicting activity of supports*
- Conclusions

Water-Assisted CVD Growth

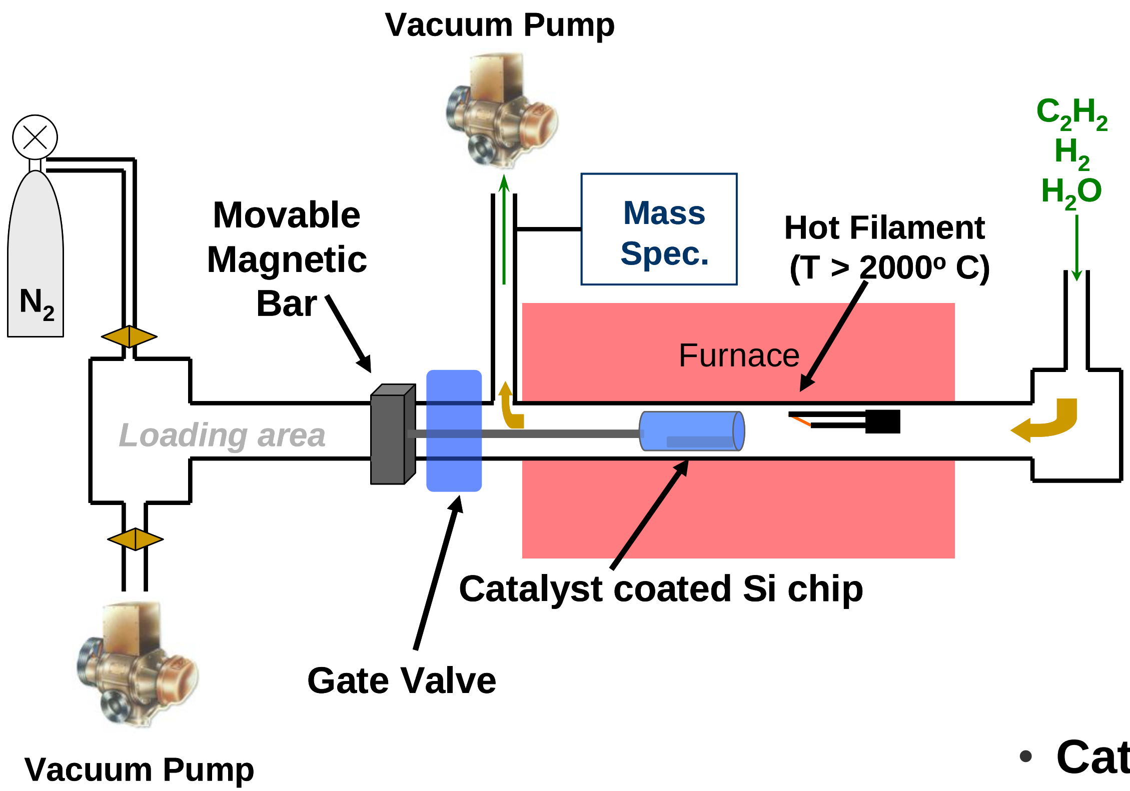

- Hot filament produces atomic hydrogen – allows rapid catalyst reduction
- Typical flow rates of precursor gases: ~ 400 sccm H_2, 2 sccm C_2H_2, and 2 sccm H_2O (at 750 °C)
- Reactor pressure = 1.4Torr

- **Catalyst support: 10nm (AlxOy)**
- **Catalyst: Fe (0.5nm)**

Pint, *et al.*, *J. Phys. Chem. C* **2009**, *113*, 4125.

Mechanisms Proposed for Growth Termination of CNTs

- Accumulation of amorphous carbon on active catalyst sites
  - Iijima, et al. *Science* **2004**, *306*, 1362; Yamada et al*. Nano Lett.* **2008**, *8*, 4288.
  - Helveg et al. *Nature* **2004**, *427*, 426.
- Formation of a silicide
  - Guggenheim, R. et al. *Appl. Phys. Lett.* **2002**, *80*, 2383
- The size of the catalyst and the stability of the carbide phase
  - Harutyunyan, A.R. et al. *Phys. Rev. Lett.* **2008**, *100*, 195502
- Chemical-mechanical coupling of the top surface of the catalyst film
  - Strano, M.S. et al. *ACS Nano* **2008**, *2*, 53

Lifetime of Catalyst

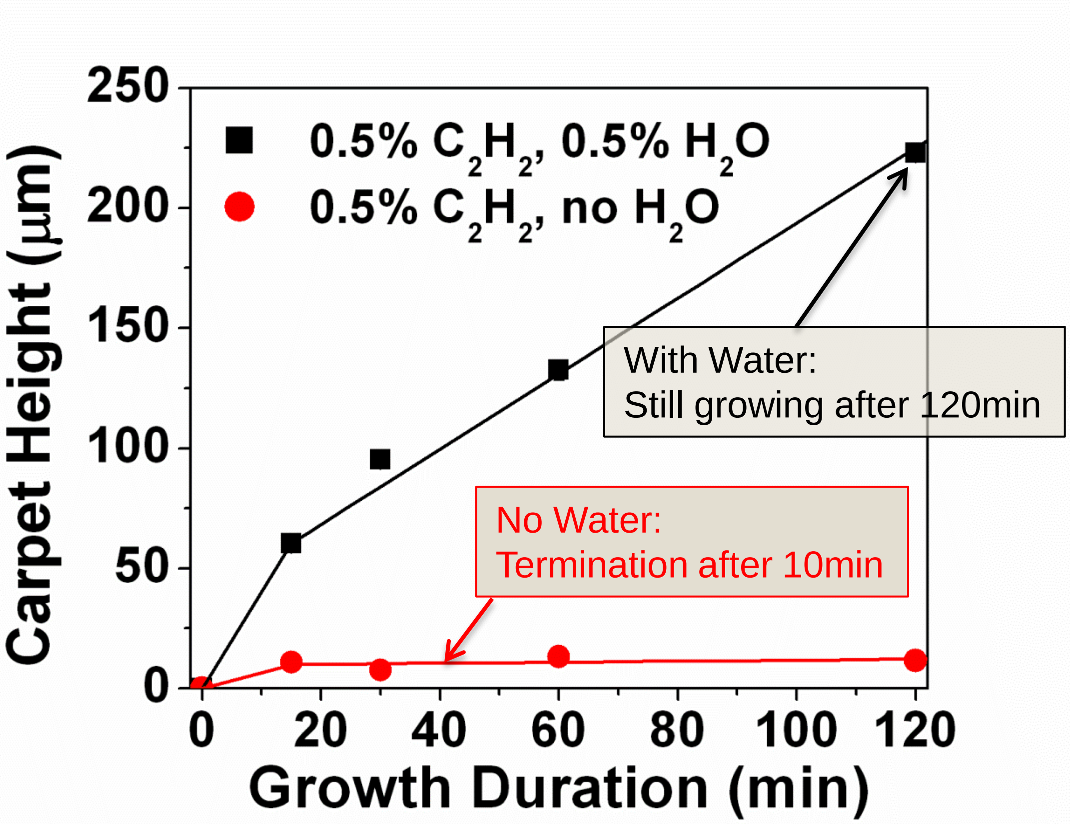

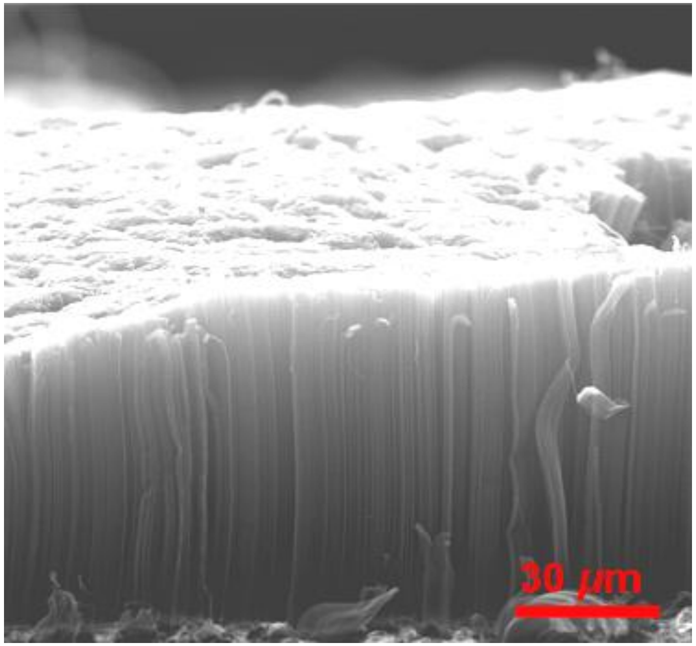

Catalysts live longer with water!

Amama, Pint, McJilton, Kim, Stach, Murray, Hauge, Maruyama, *Nano Lett.* **2009**, *9*, 44.

Ostwald Ripening (OR)

- Ostwald ripening is the phenomenon by which size inhomogeneity in a particle distribution is magnified over time
- Large particles increase in size at the expense of smaller particles via atomic interdiffusion
- Number density decreases, avg. diameter increases
- The driving force for Ostwald ripening is the reduction of surface energy

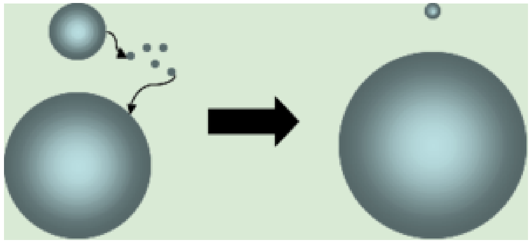

Graphic from Wikipedia.org

Wilhelm Ostwald

Discovered OR in 1896

5-eV LEEM images of the coarsening of Au catalyst droplets on Si(111) at 600 °C

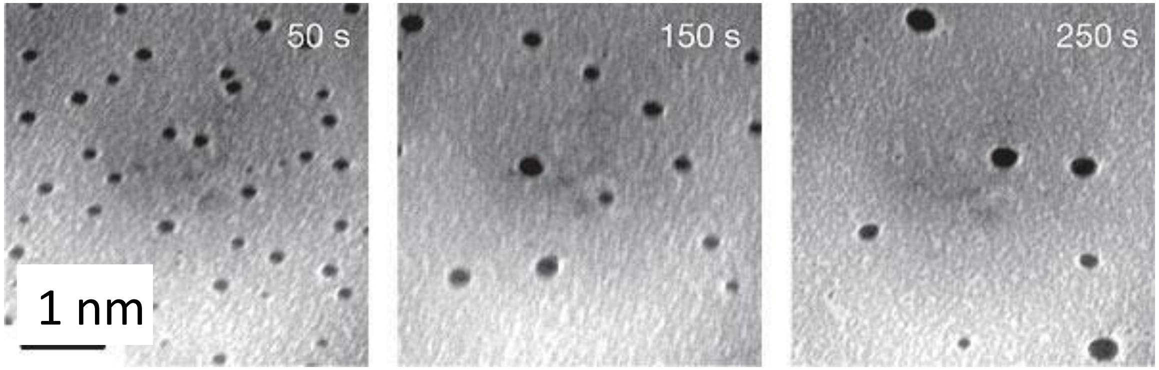

The number of droplets decreases with time as larger droplets grow at the expense of smaller ones

The influence of the surface migration of gold on the growth of silicon nanowires

Hannon, Kodambaka, Ross, Tromp, *Nature*, **2006**, *440*, 69-71.

Effect of Water on Ostwald Ripening Rate

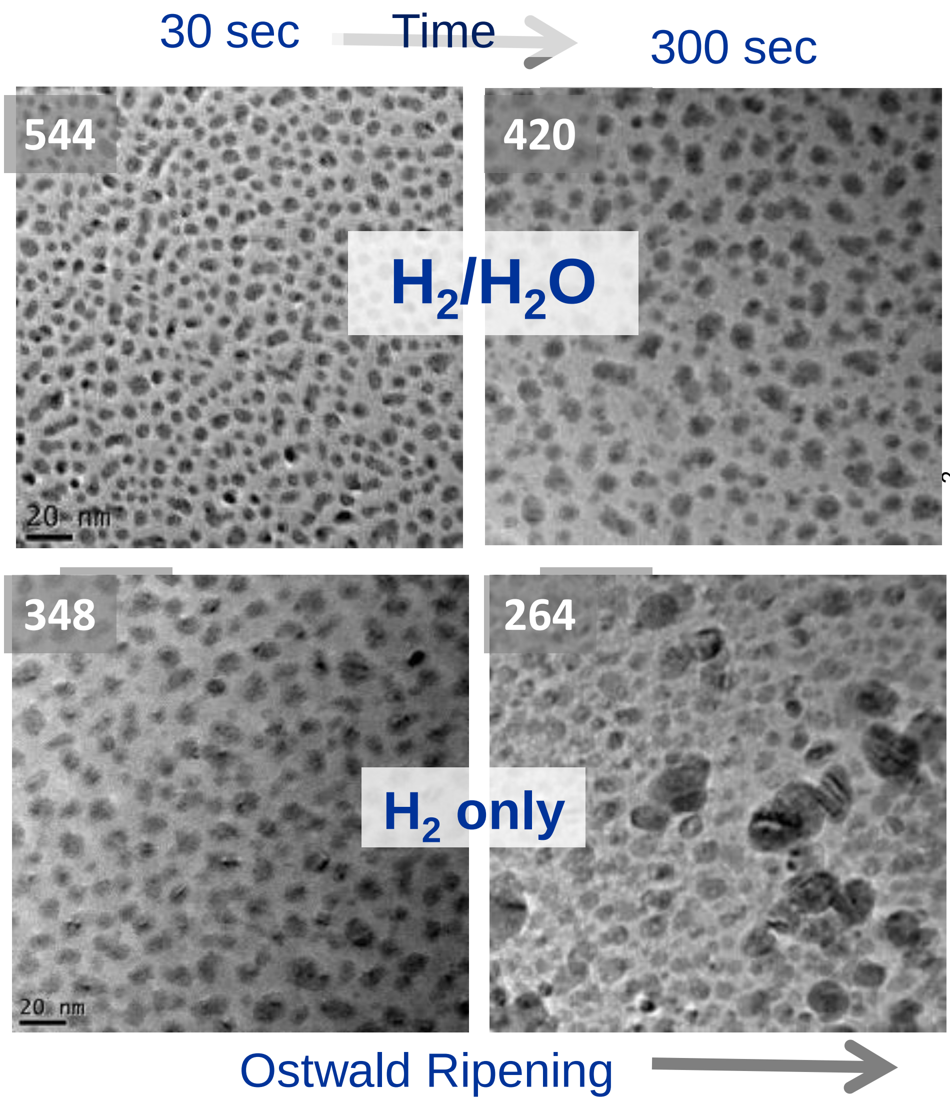

Water impedes Ostwald Ripening

Higher number density (200 nm)^2 of nanoparticles indicates that water impedes Ostwald ripening

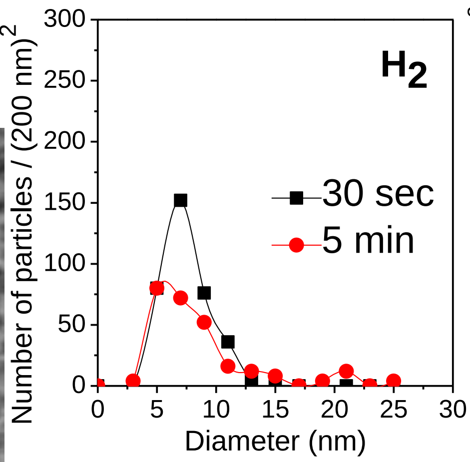

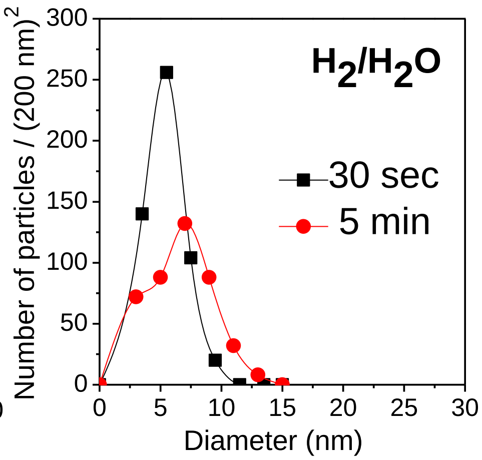

Amama et al., *Nano Lett.* **2009**, *9*, 44.

Catalyst Particles Formed After Thermal Annealing

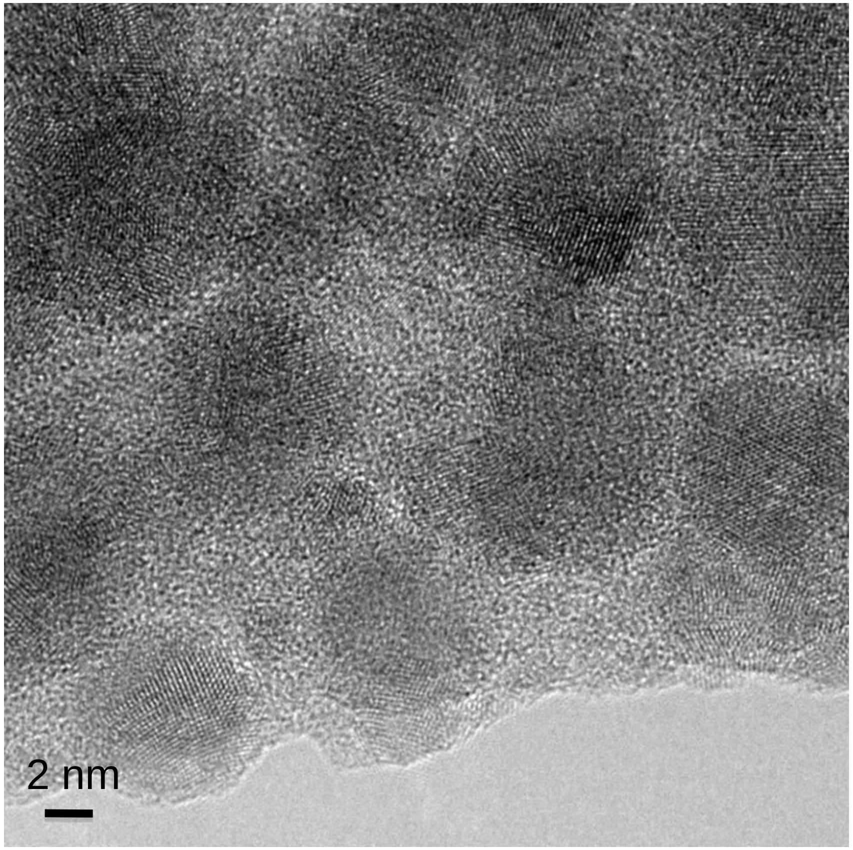

H_2 (5 min)

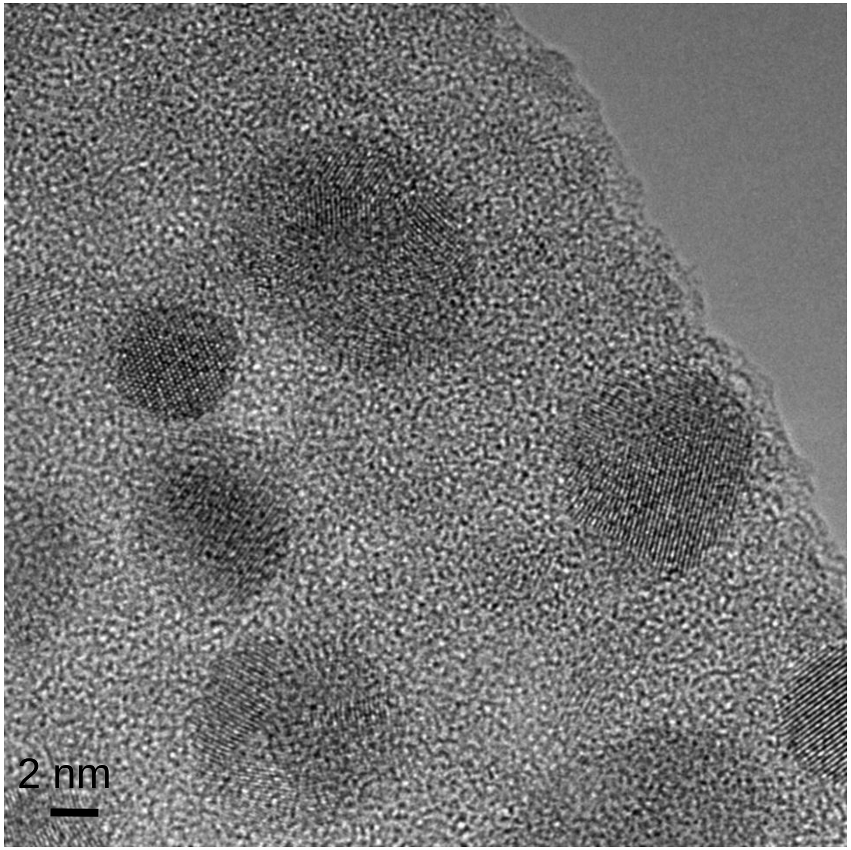

H_2+H_2O (5 min)

Water preserves particles that have sizes less than 6nm; 5-6nm Fe_2O_3 particles correspond to Fe particles in the range of 3-4 nm; SWCNT mean diameter is ~3 nm

Catalyst Nanoparticles Formed After Thermal Annealing

AFM topography images of Fe_2O_3 nanoparticles

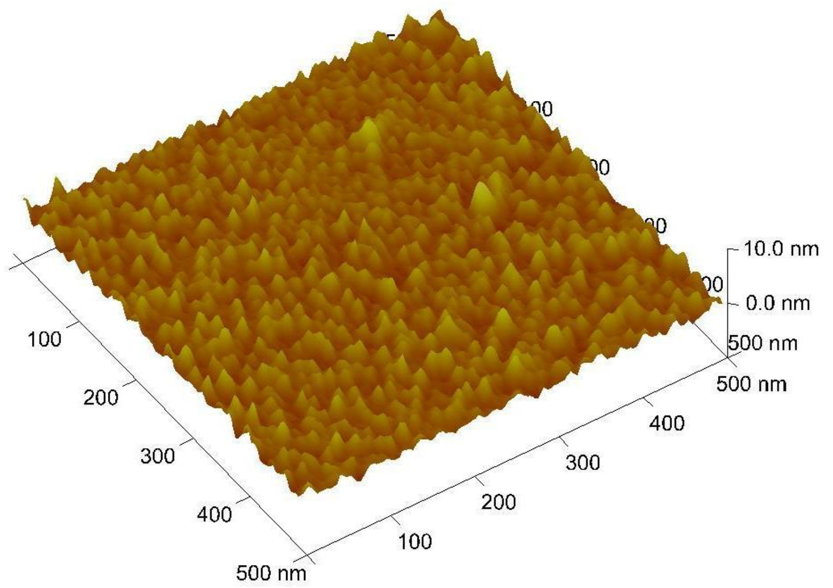

H_2, 5 min

Mean feature height = 3.5 nm

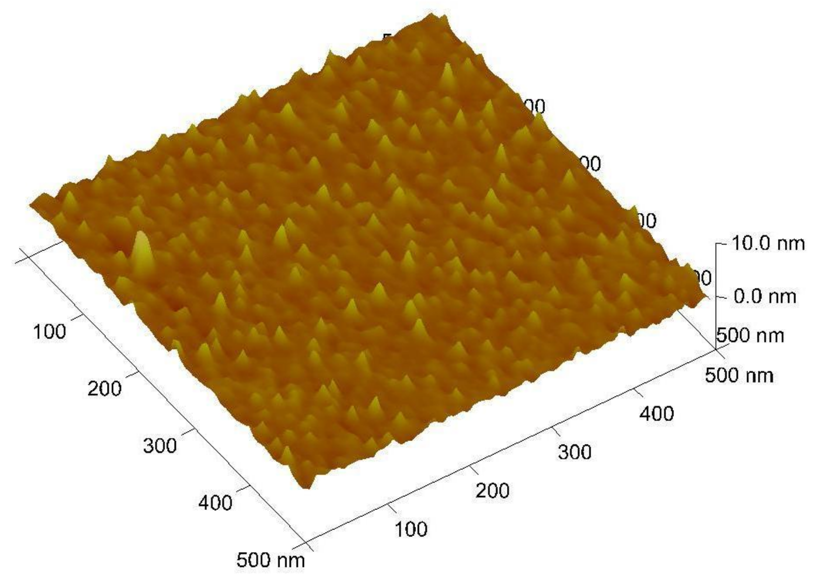

H_2+H_2O, 5 min

Mean feature height = 2.6 nm

Amama, Pint, McJilton, Kim, Stach, Murray, Hauge, Maruyama, *Nano Lett.* **2009**, *9*, 44.

Exposed Catalyst Layer After SWCNT Growth

- Following growth for 30s in C_2H_2
- Again, clear signs of Ostwald ripening, but is limited for the H_2O case

Amama, *Nano Lett.* **2009**, *9*, 44.

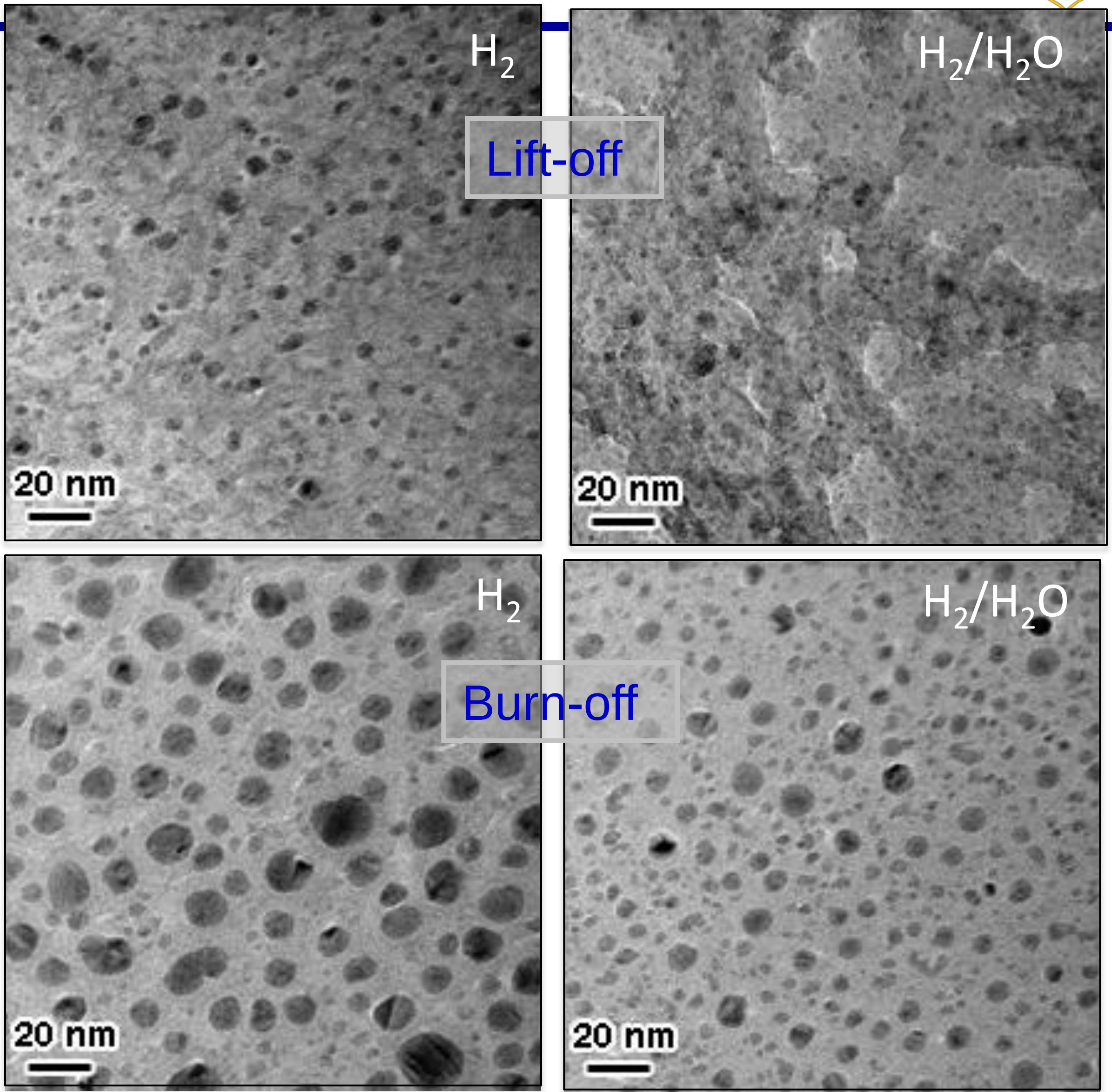

Growth Termination Mechanism

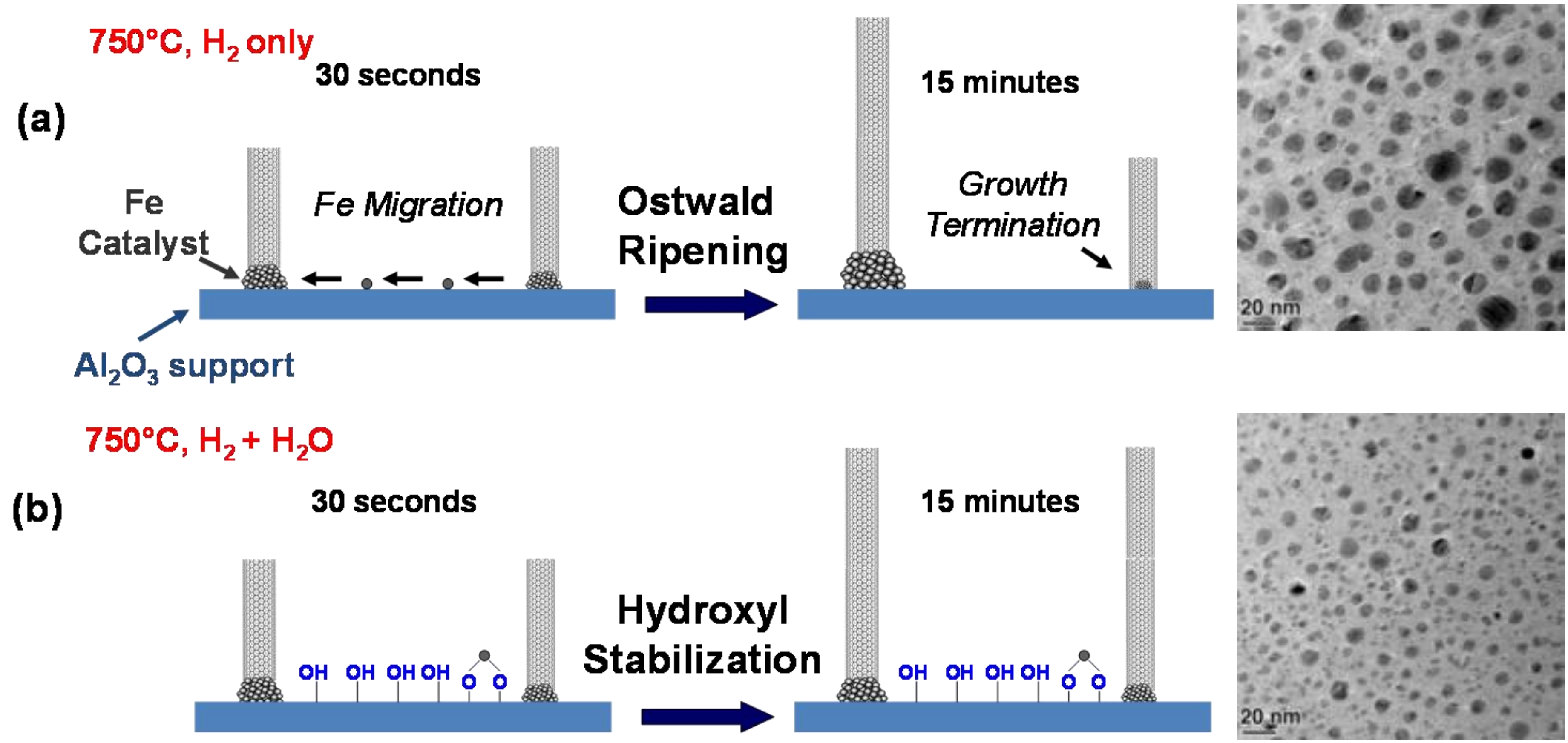

Amama, Pint, McJilton, Kim, Stach, Murray, Hauge, Maruyama, *Nano Lett.* **2009**, *9*, 44.

Thermal Annealing : 750°C in H_2/H_2O

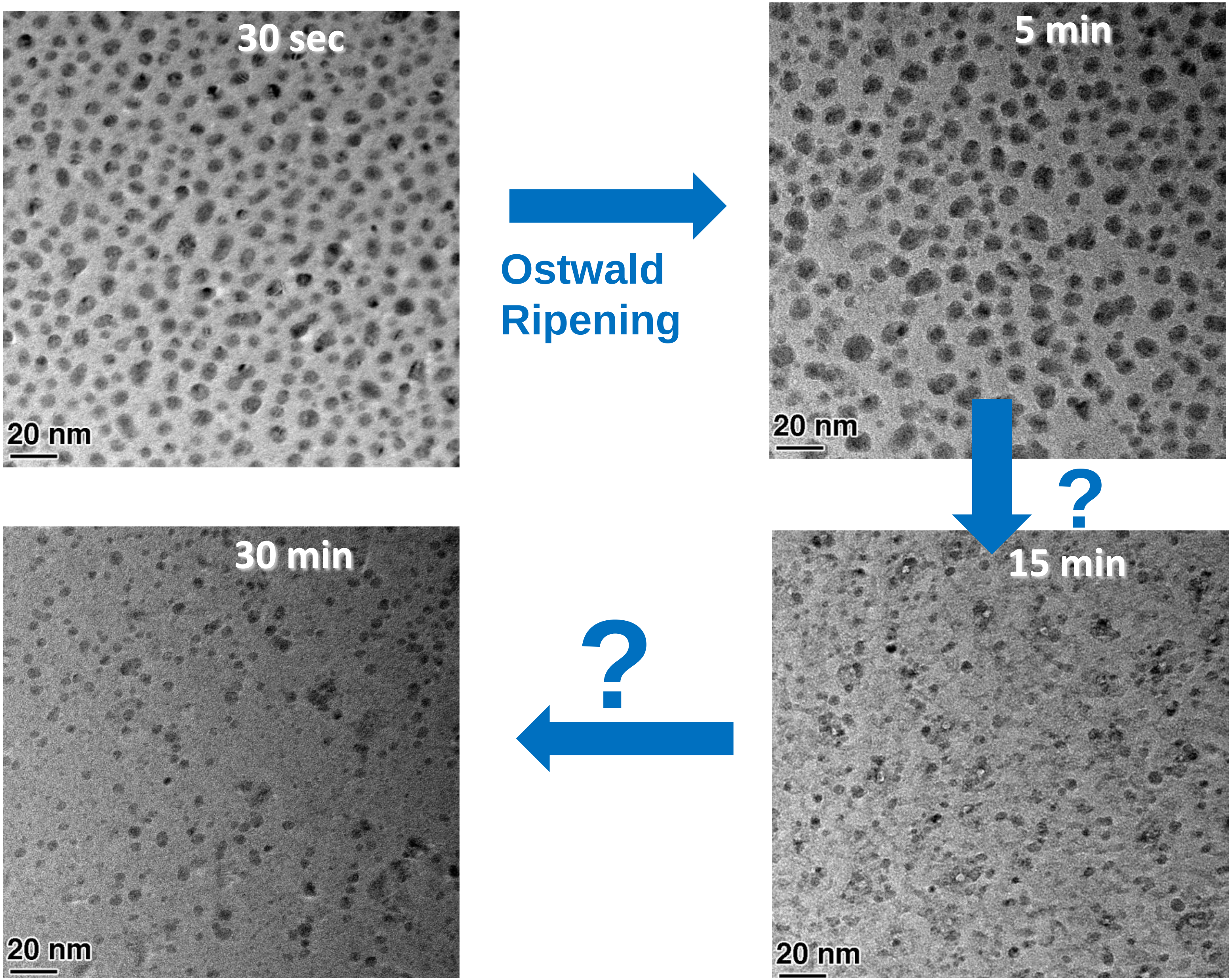

Amama, Pint, McJilton, Kim, Stach, Murray, Hauge, Maruyama, *Nano Lett.* **2009**, *9*, 44.

Thermal Annealing : 750°C in H_2/H_2O

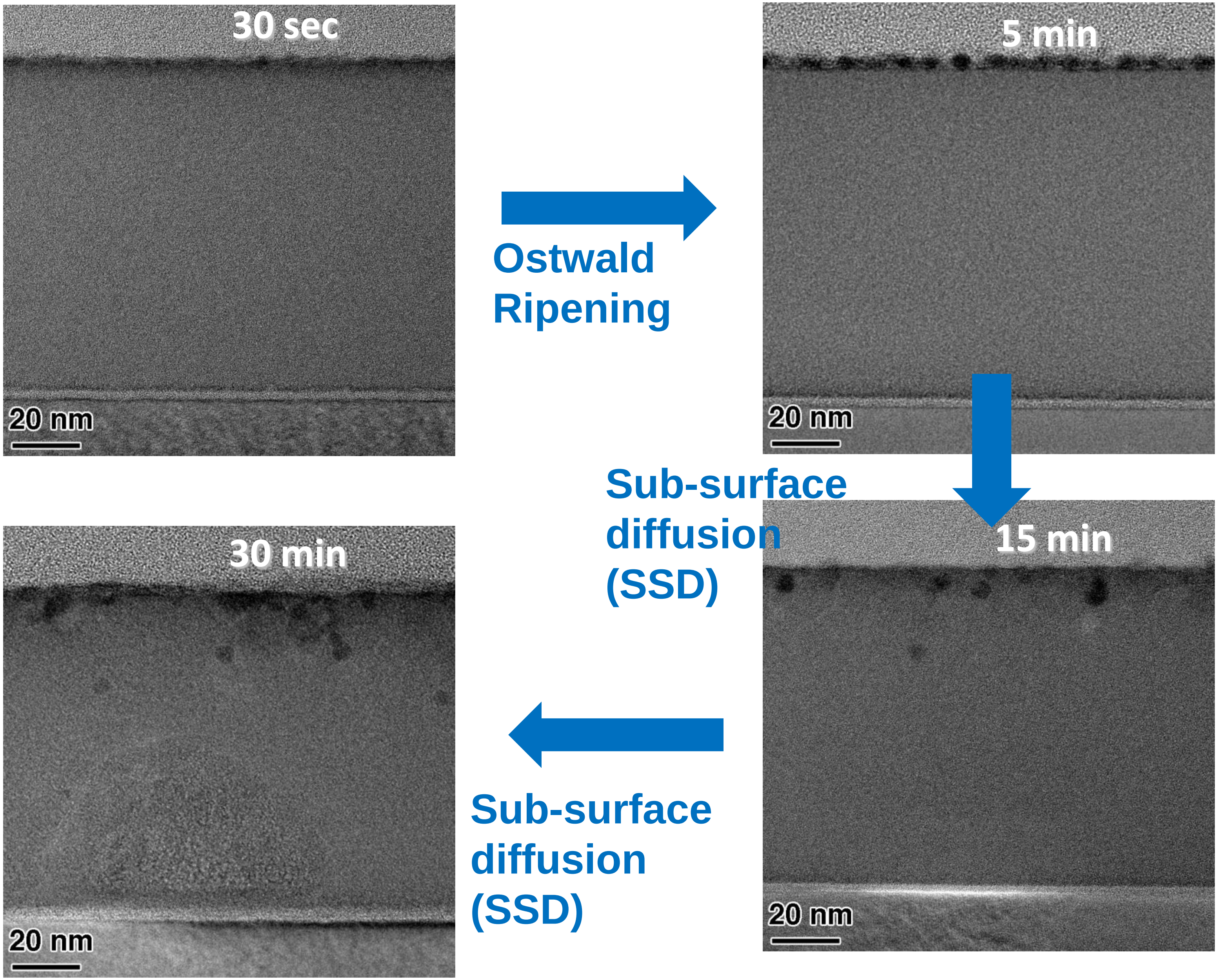

Kim, Pint, Amama, Zakharov, Hauge, Maruyama, Stach, *J. Phys. Chem. Lett.* **2010**, *1*, 918.

Mass Loss via OR and SSD

- Ostwald ripening dominates in the early part of growth
- Not only is ripening observed, but we also observe Fe loss …
- Both phenomena may be intrinsically linked to the growth process
- Fe migration into a more stable, high-coordination bulk site
- Atomic Fe diffuses into the alumina and form particles in pores
- Diffusion of catalyst will cause mass loss from the catalyst that grow CNTs causing termination

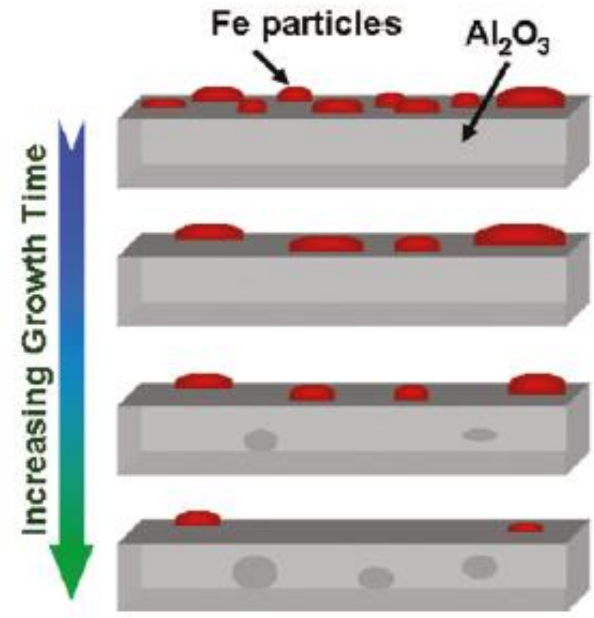

Kim, Pint, Amama, Zakharov, Hauge, Maruyama, Stach, *J. Phys. Chem. Lett.* **2010**, *1*, 918.

Reinterpretation of Previous Works via Ostwald Ripening

- Gas environment: Extended reduction in hydrogen leads to excessive coarsening (rapid insertion, water, atomic hydrogen, low H_2 conc.)
- Molybdenum used in steels to impede Ostwald ripening (Resasco's CoMoCat)
- Action of ferrocene may be to resupply Fe to shrinking catalysts, keeping them large enough to continue growth

Summary (I)

- Ostwald ripening has been demonstrated to be reduced under supergrowth conditions
- The extended lifetime of supergrowth catalysts can thus be explained by the decreased rate of Ostwald ripening / coarsening through the ability of oxygen and hydroxyl species to reduce migration of catalyst atoms
- We propose that growth stops as Ostwald ripening and subsurface diffusion deplete the catalyst
- The reduction in the number of particles observed during heat treatment correlates with the number of CNTs that stop growing
- **Dynamic catalyst evolution during growth contributes to growth termination**

Outline

- Motivation and overview
- Role of water and growth termination
  - *Ostwald ripening & subsurface diffusion phenomena*
- Influence of support-metal interactions (SMI)
  - *Carpet growth (catalyst activity & lifetime)*
  - *3D evolution of the catalyst*
- Features of a good catalyst support
  - *Porosity*
  - *Active site density*
  - *Powerful tool for predicting activity of supports*
- Conclusions

Influence of Catalyst Support

- Stability and activity of catalyst during SWCNT carpet growth is sensitive to the properties of the support
- Co catalyst supported on different crystal faces of Al_2O_3 (A-, R- and C-faces) shows different catalyst behavior
  - Ohno et al. *Jpn. J. Appl. Phys.* **2008**, *47*, 1956.
- Co-Mo catalyst supported on different supports produces SWCNTs with different *(n,m)* selectivity
  - Wang, Li, & Chen, *J. Mater. Sci.* **2009**, *44*, 3285.
- Fe catalyst (<0.6nm) supported on SiO_2, Al_2O_3 and Al_2O_x, shows different growth behaviors
  - Noda et al. *Jpn. J. Appl. Phys.* **2007**, *46*, L399.

CVD Growth of SWCNT Carpets

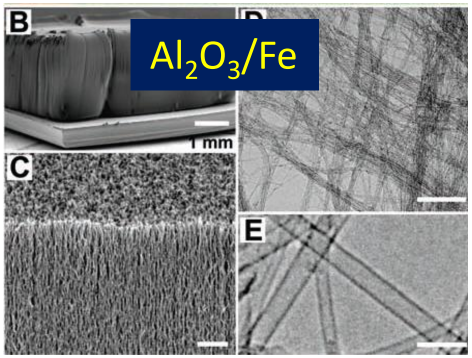

Hata et al., *Science* **2004**

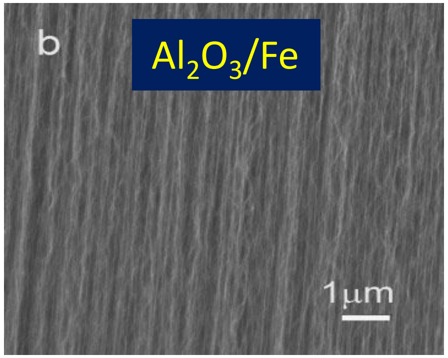

Li et al., *Adv. Mater.* **2006**

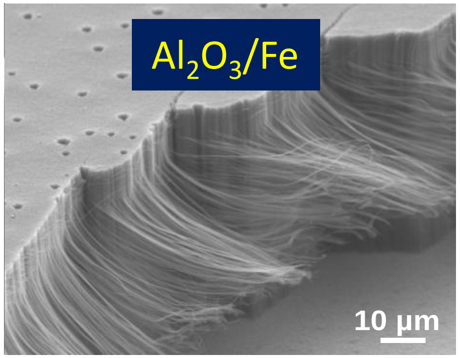

Pint et al., *JPC C* **2009**

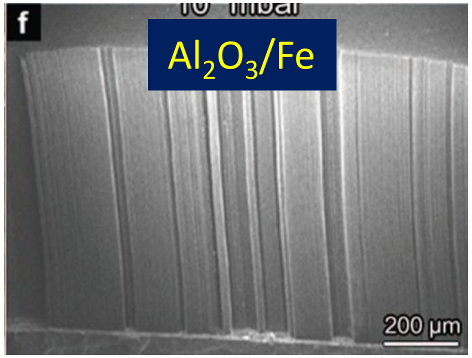

Mattevi et al., *JPC C* **2008**

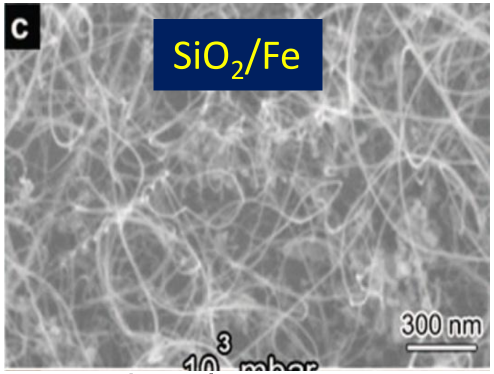

Mattevi et al., *JPC C* **2008**

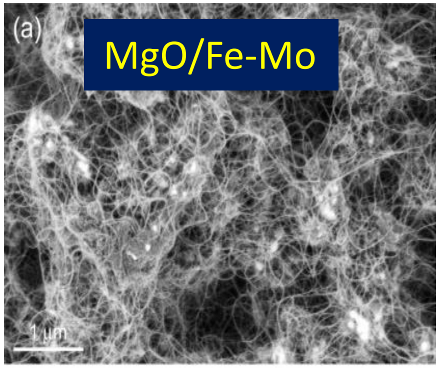

Yoshihara et al., *JPC C* **2008**

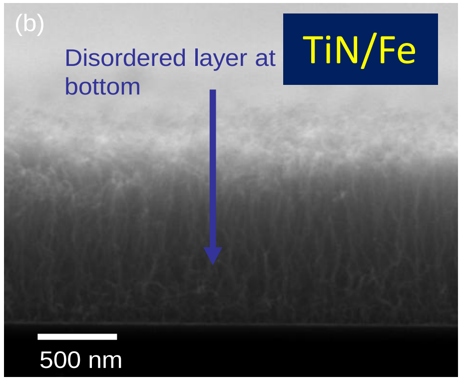

Amama et al., *Carbon* **2012**

- The catalyst commonly used for SWNT carpet growth: Al_2O_3 (10-200nm)/Fe (< 1 nm)
- Other supporting layers (SiO_2, TiN, MgO and ZrO_2) do not appear to support aligned SWNT growth

Why is Alumina a Good Support?

- Al_2O_3/Fe provides increased CNT nucleation density (Mattevi *et al. J. Phys. Chem. C* **2008**, *112*, 12207)
- Alumina is able to reduce Ostwald ripening due to the stronger catalyst-substrate interaction
- The chemical similarity between Fe^{3+} and Al^{3+} partly accounts for the strong interaction (Sushumna and Ruckenstein *J. Catal.* **1985**, *90*, 4726)
- Alumina helps to preserve the Fe (111) crystallographic planes that are known to have high catalytic activity and inhibit the less active Fe (100) and (110) planes (Sormorjai *et al. J. Phys. Chem.* **1986**, *90*, 4726)

Different Types of Alumina

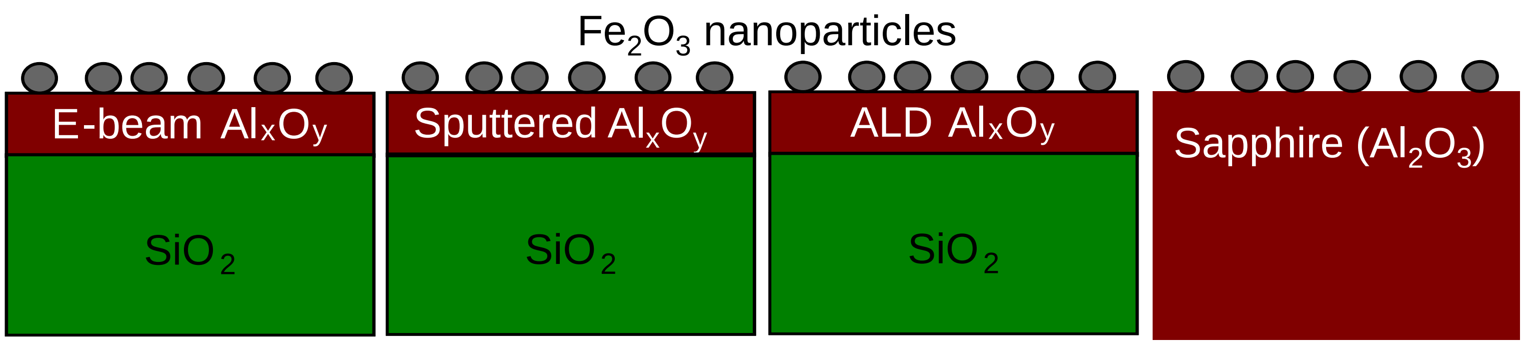

Thickness of AlxOy film: 10 nm

- **E-beam:** particles deposited have limited mobility; more lacunas
- **Sputtering:** powerful electron bombardment; higher defect density
- **ALD:** slow; well-controlled; atomic layers deposited sequentially
- Sapphire; c-cut single crystal [0001]

FESEM Characterization

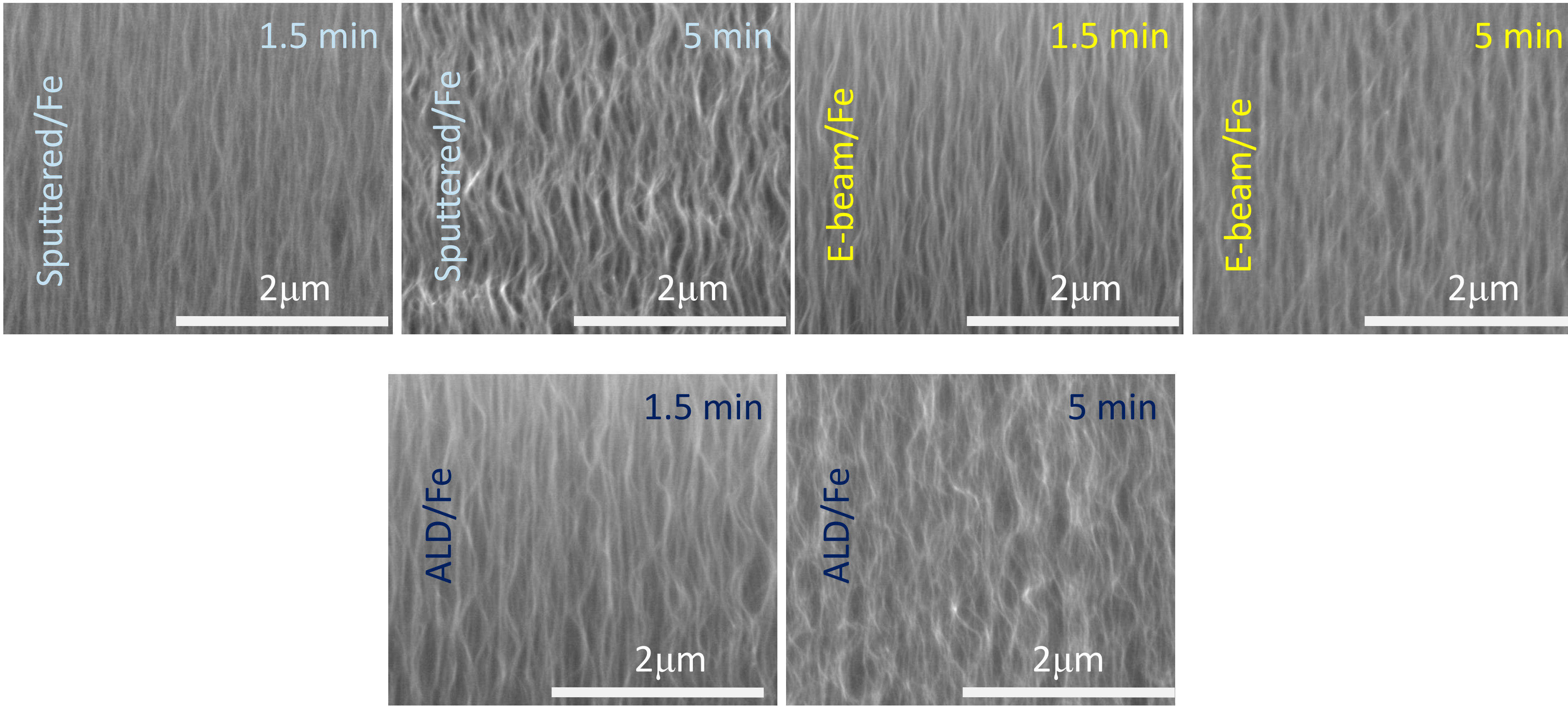

Amama, Pint, Kim, McJilton, Eyink, Stach, Hauge, Maruyama, *ACS Nano* **2010**, *4*, 895.

Effect of Alumina Type on Catalyst Activity

- There is a strong dependence of the SWCNT carpet height on the type of alumina used as support
- Sputtered/Fe supports a faster growth rate and shows the longest life time followed by e-beam/Fe
- Annealed e-beam/Fe results in early growth termination
- Sapphire/Fe does not support carpet growth

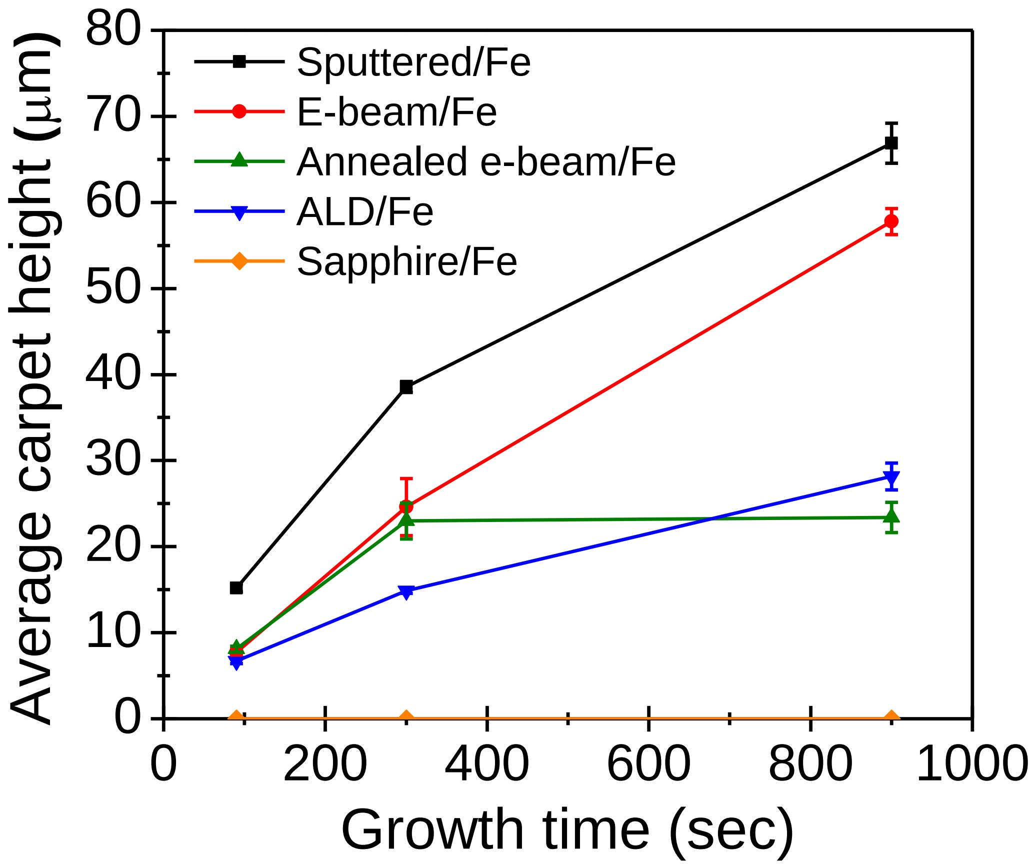

Catalyst activity: sputtered/Fe > e-beam/Fe > ALD/Fe > sapphire/Fe

Amama, Pint, Kim, McJilton, Eyink, Stach, Hauge, Maruyama, *ACS Nano* **2010**, *4*, 895.

Raman Spectroscopy

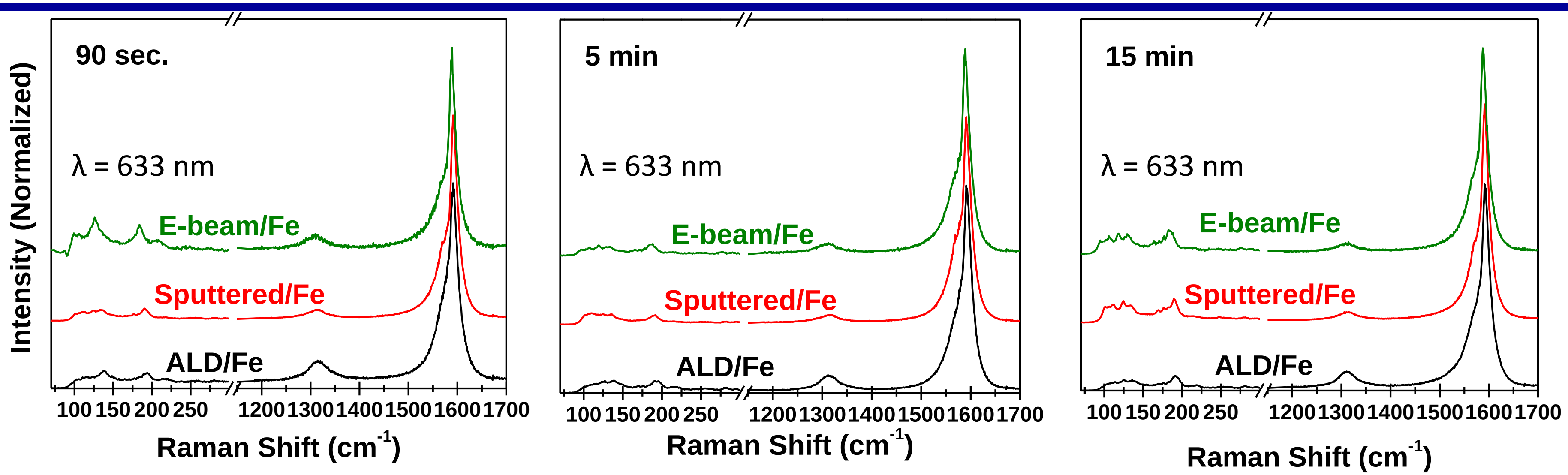

Catalyst	G/D (1.5 min)	G/D (5 min)	G/D (15 min)
ALD/Fe	9.89	13.32	12.02
Sputtered/Fe	**22.0**	**28.88**	**29.17**
E-beam/Fe	13.63	18.29	20.0
Sapphire/Fe	3.04	1.97	N/A

Amama, Pint, Kim, McJilton, Eyink, Stach, Hauge, Maruyama, *ACS Nano* **2010**, *4*, 895.

Catalyst Evolution in the Absence of C_2H_2

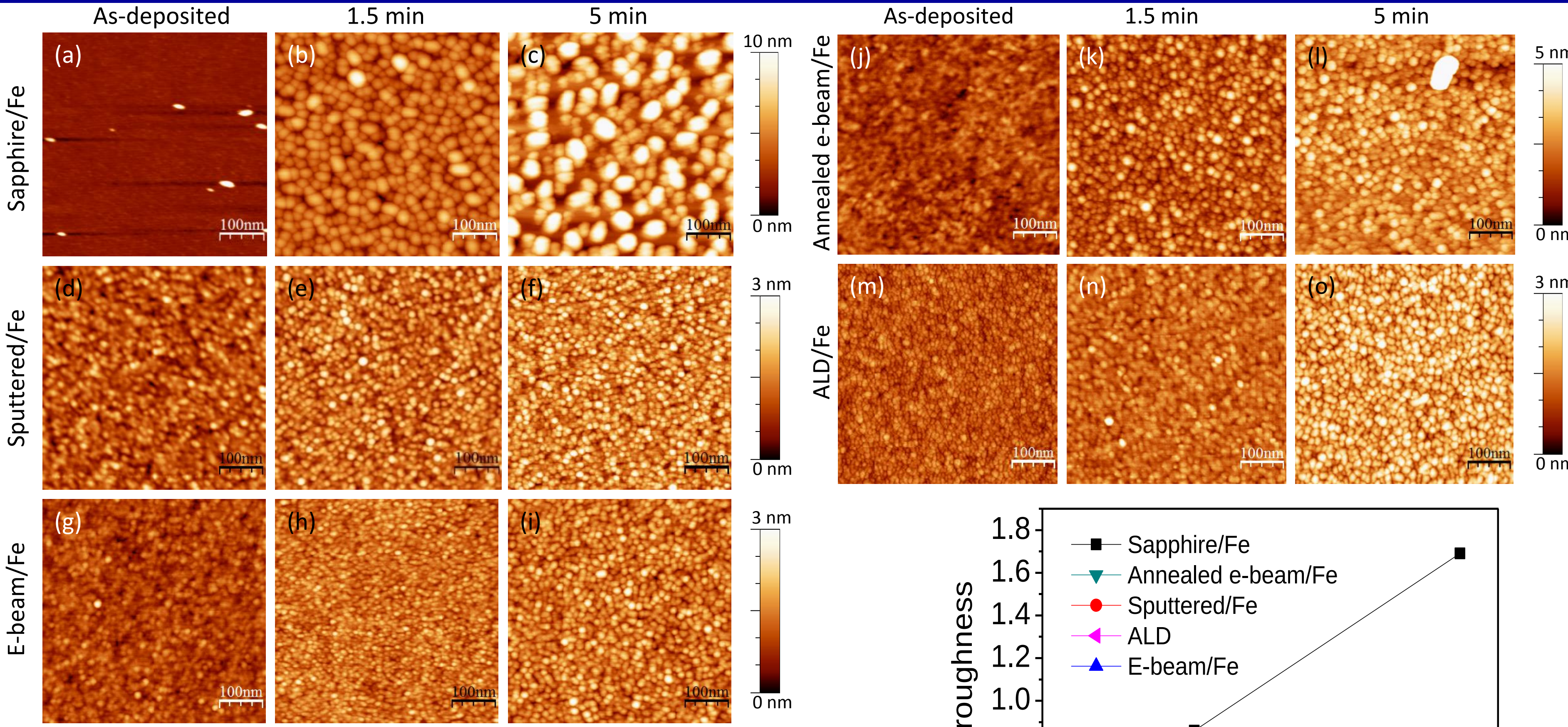

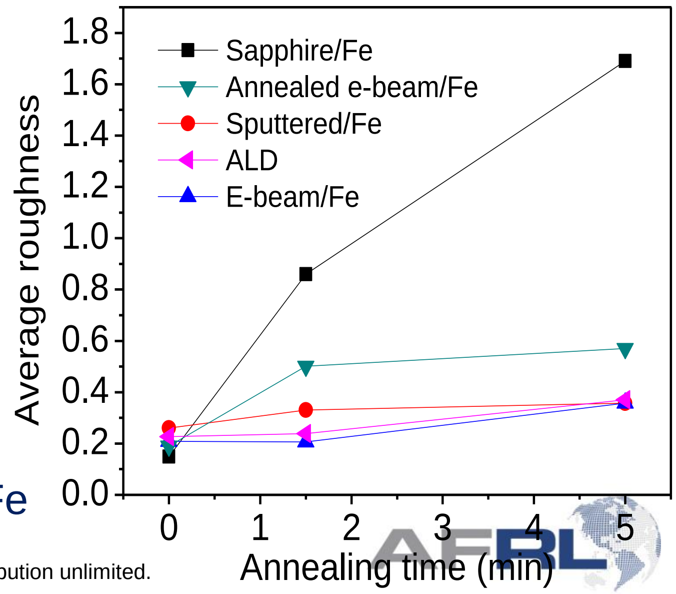

Roughness ratio between 5 and 0 min:
Sapphire/Fe>Annealed/Fe>ALD/Fe Ebeam/Fe>Sputtered/Fe

Catalyst Nanoparticles Formed on Different Alumina Types

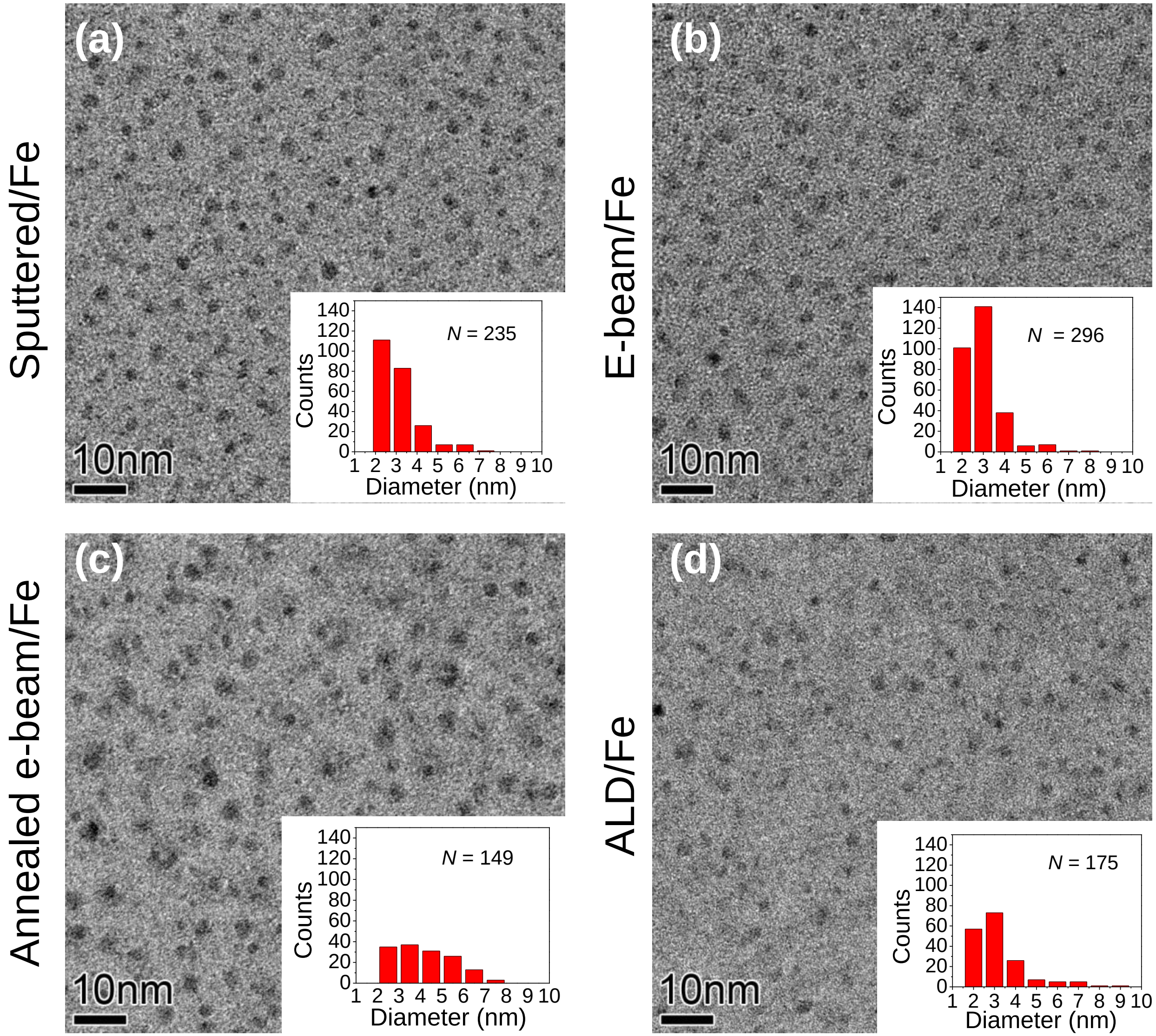

Plan-view TEM images of Fe particles formed on the different alumina flavors after exposure to growth conditions in the absence of C_2H_2 for 15min

Inset histograms: PSDs and *N* in a 100 × 100 nm^2 area

Sputtered/Fe and e-beam/Fe have higher number density

Annealed e-beam/Fe is characterized by severe OR

Amama, et al., *ACS Nano* **2010**, *4*, 895

XPS Sputter Depth Profile Analysis

- Samples were sputtered for cycles of 15 sec using Ar^+ with KE = 1 KeV
- Each sputtering step was estimated to produce a depth of ~0.5 nm
- The catalyst evolution is analyzed on the basis of the ratio of the integrated peak areas of Fe $2p_{3/2}$ and Al 2p as a function of sputtering time.
- The inward diffusion of Fe in alumina increases in the following order: sapphire/Fe < annealed/Fe < ALD/Fe < sputtered/Fe < e-beam/Fe.

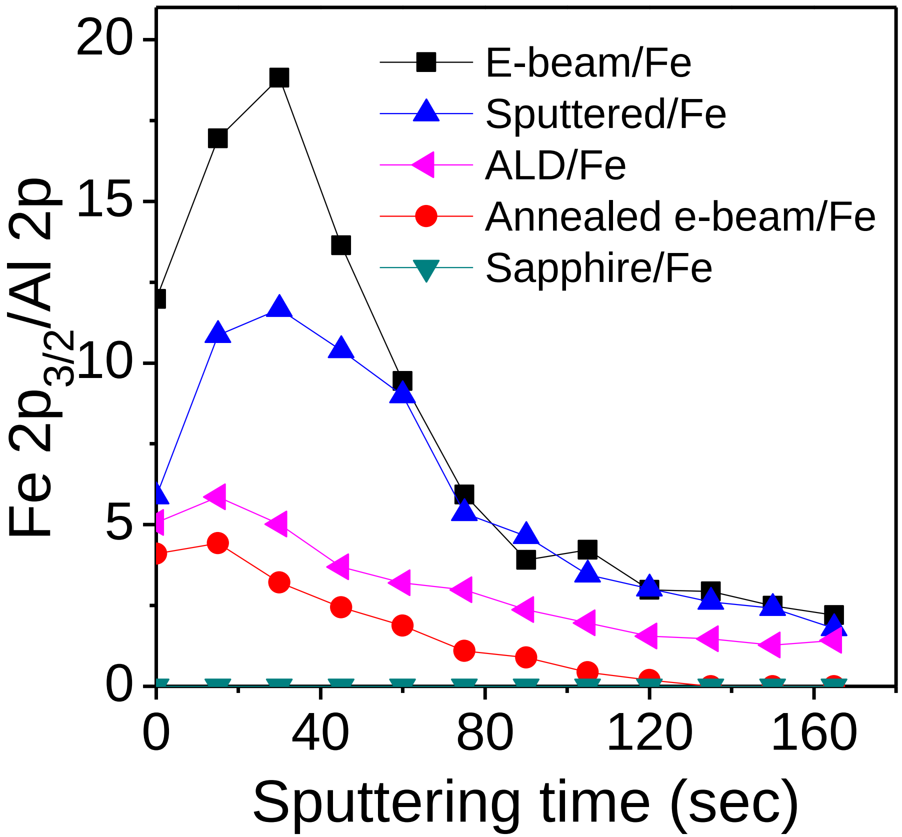

Amama, Pint, Kim, McJilton, Eyink, Stach, Hauge, Maruyama, *ACS Nano* **2010**, *4*, 895

Subsurface Diffusion of Fe

Cross-sectional TEM images of exposed catalysts after SWCNT carpet growth for 15 min

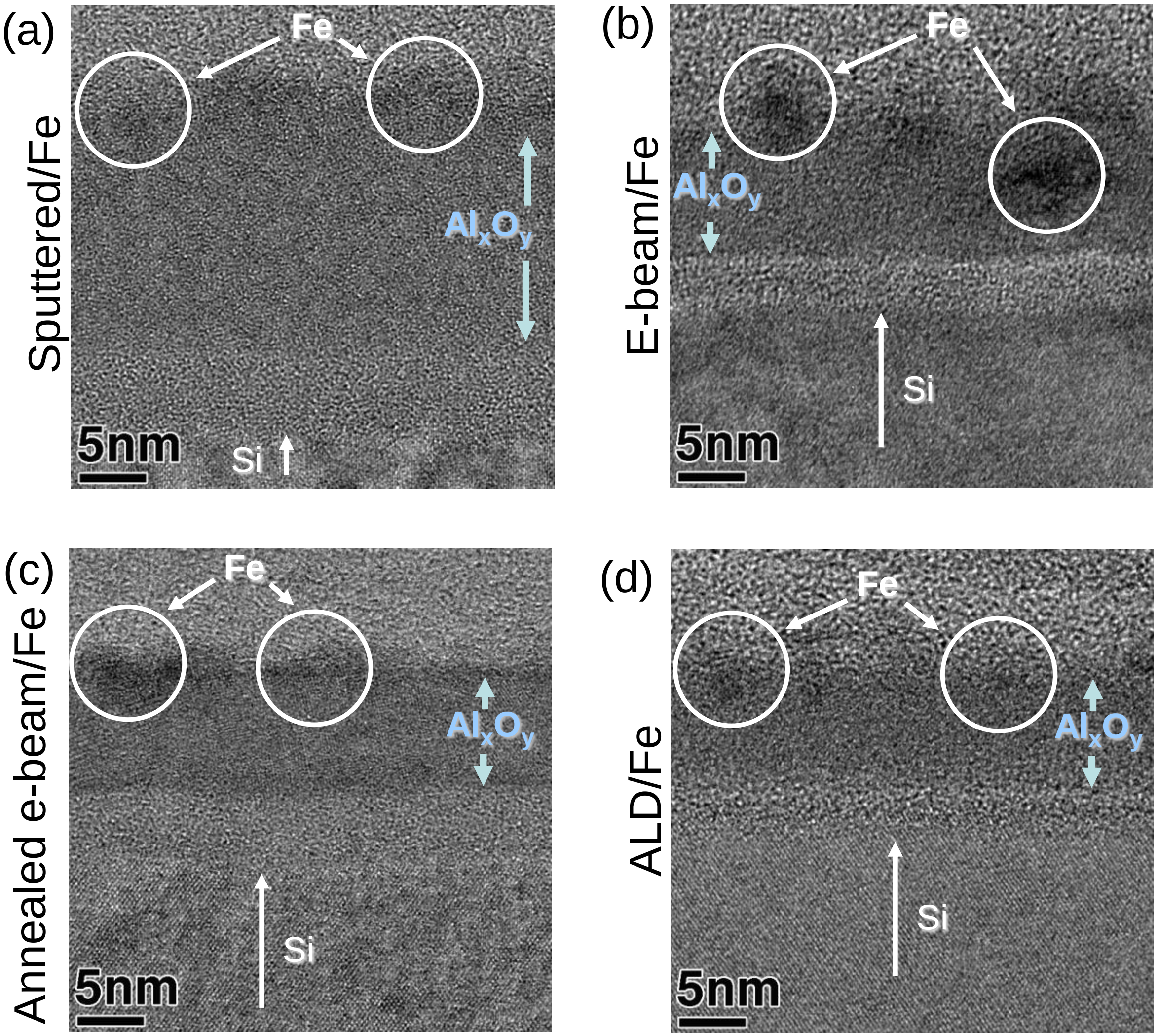

There is high inward diffusion rate of Fe in e-beam/Fe as catalyst particles can be observed below the surface

Catalysts are only observed on the surface of for the other alumina-supported catalysts

Amama, et al., *ACS Nano* **2010**, *4*, 895.

Variable Angle of Incidence Spectroscopic Ellipsometry (VASE)

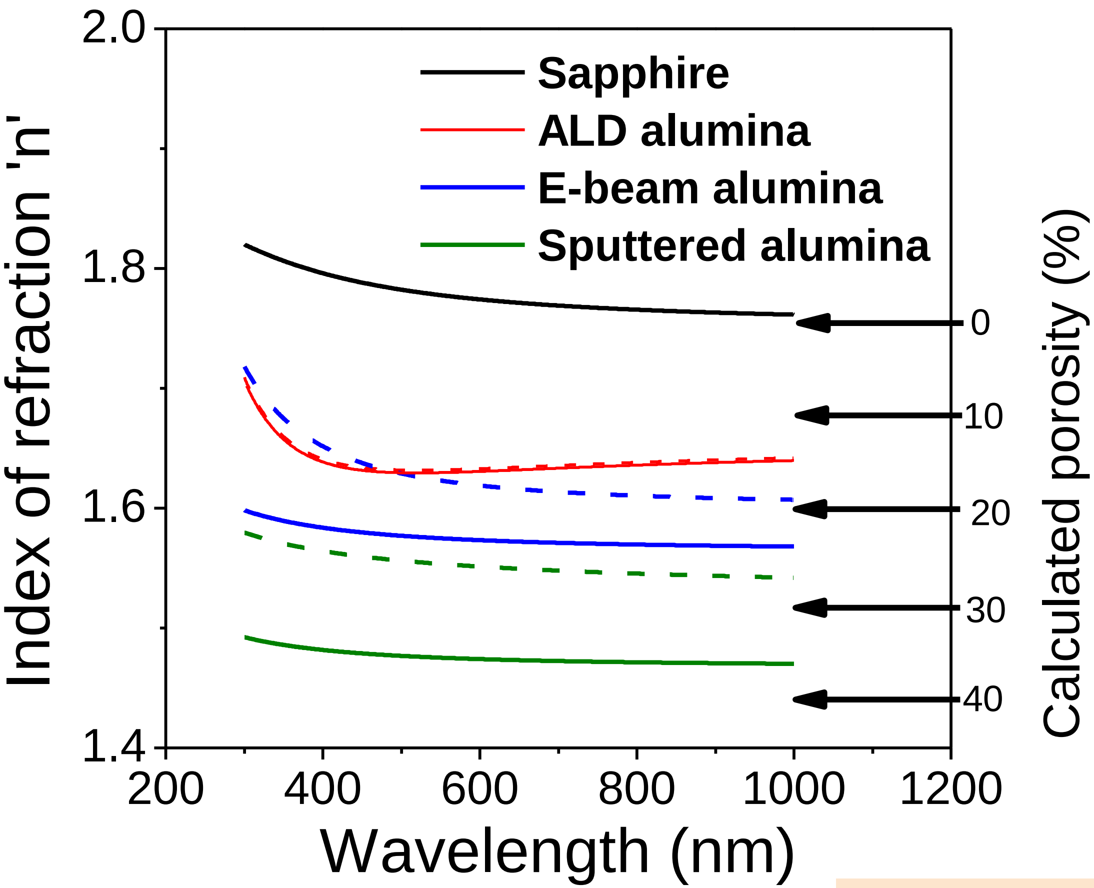

Solid lines: Pristine alumina samples

Dashed lines: After thermal annealing at 750°C for 15 min

Porosity & catalyst activity:
Sapphire < ALD < e-beam < sputtered

Amama, Pint, Kim, McJilton, Eyink, Stach, Hauge, Maruyama, *ACS Nano* **2010**, *4*, 895.

Relationship Between Catalytic Activity, OR Rate, and Porosity

Ostwald Ripening (OR) Rate, Alumina Porosity, & Carpet Height

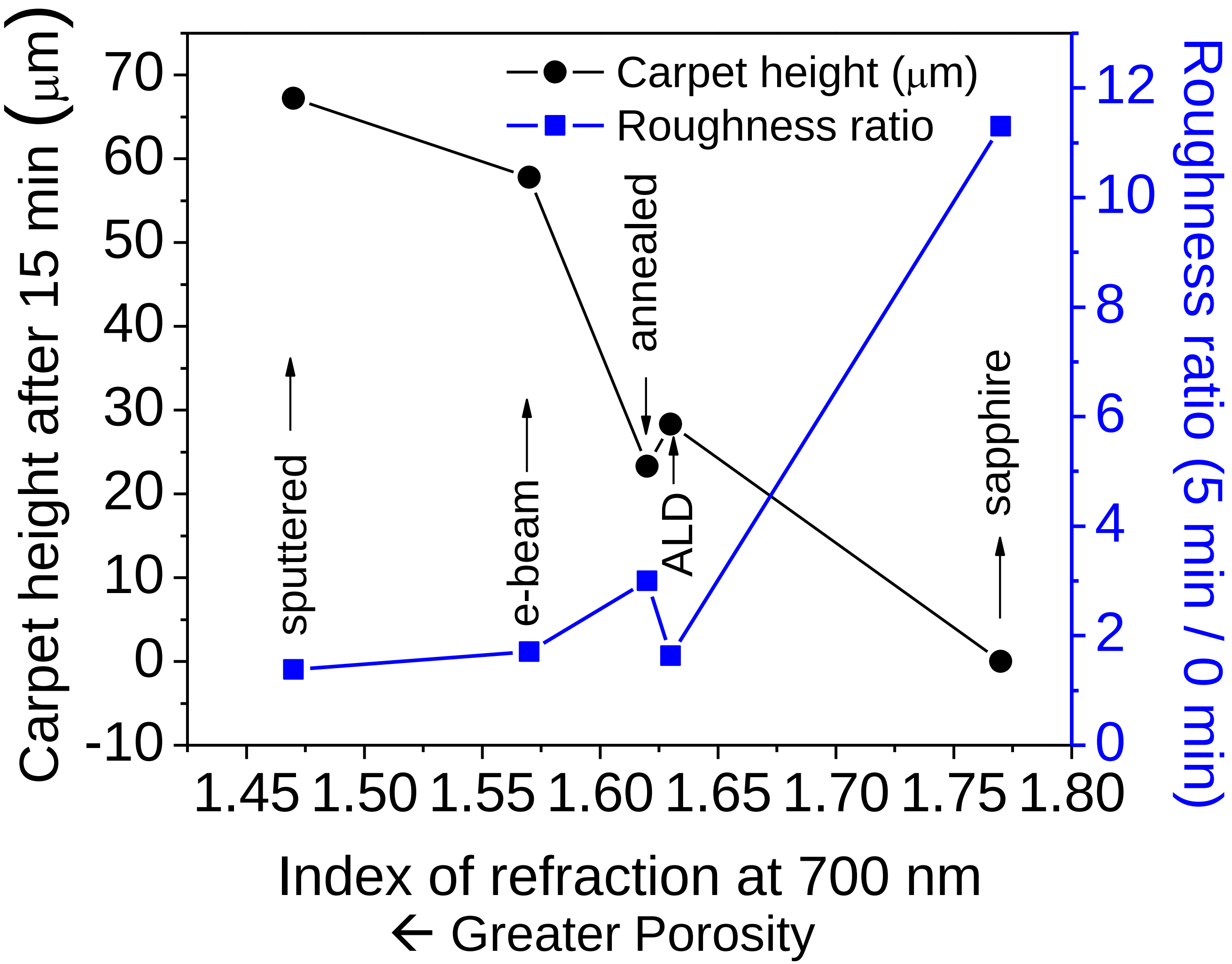

Relationship Between Catalytic Activity, SSD, and Porosity

Subsurface Diffusion (SSD), Alumina Porosity, & Carpet Height

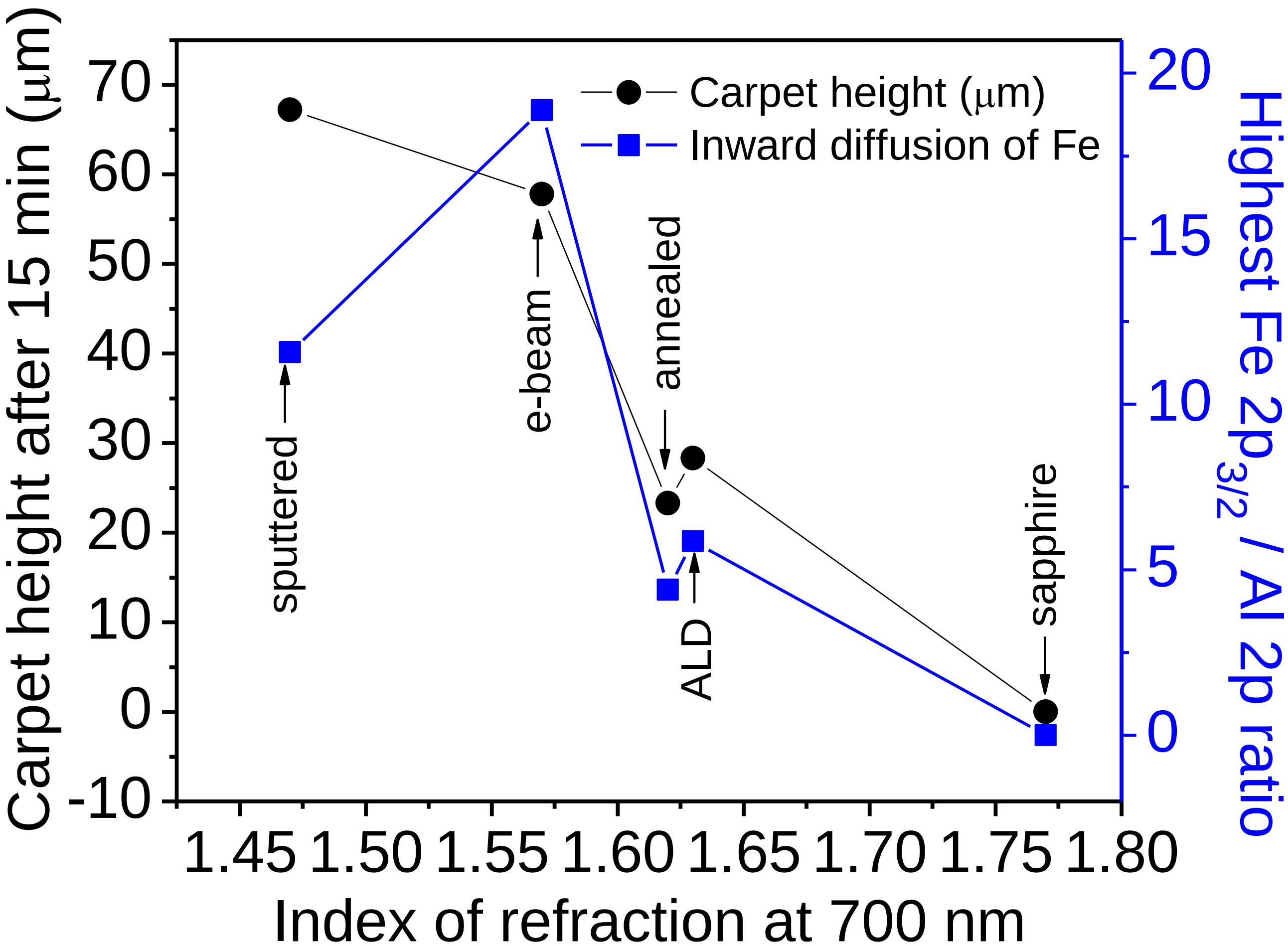

← Greater Porosity

Subsurface Diffusion of Fe

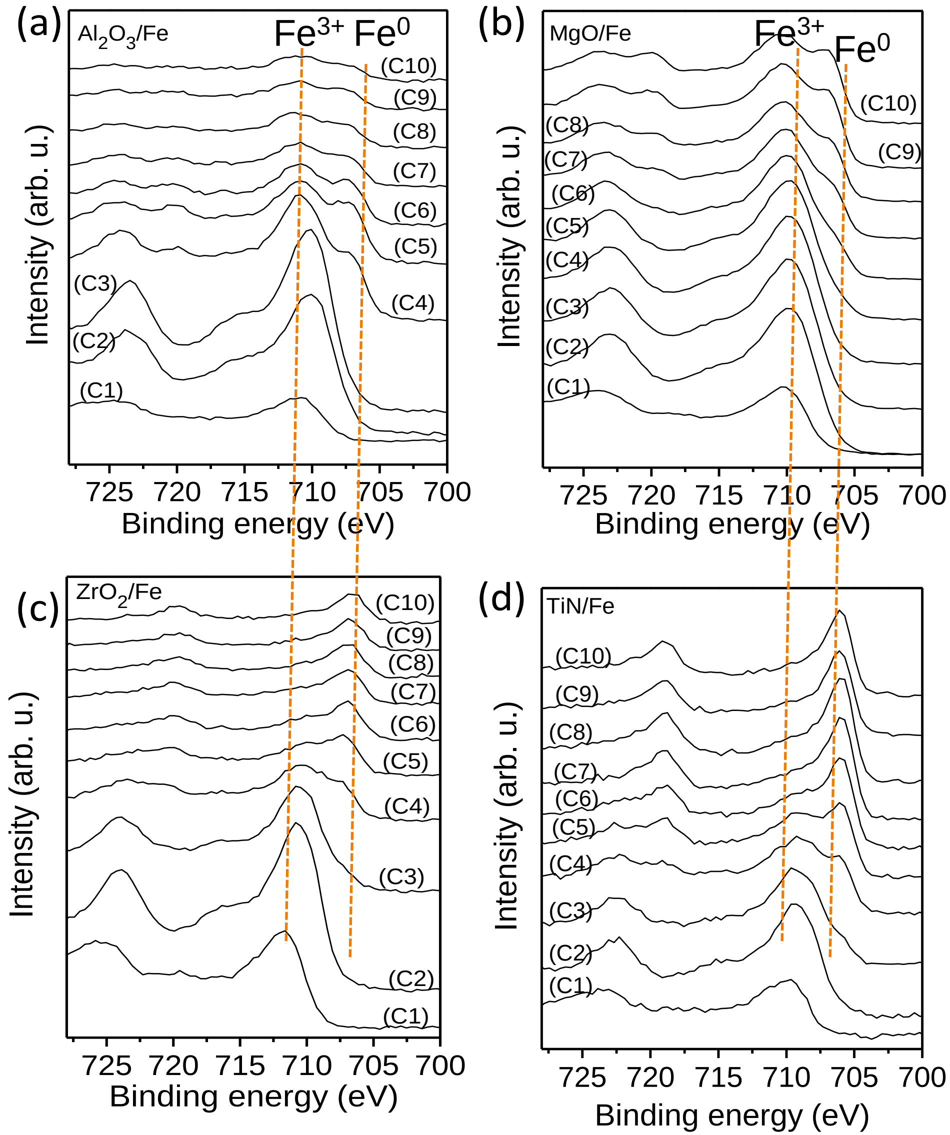

- Ex situ XPS depth profile of samples after 5 min anneal
- Evolution of the Fe 2p core line for Al_2O_3/Fe, MgO/Fe, ZrO_2/Fe and TiN/Fe after sputter-etching for 10 cycles (depth of 5 nm)
- Fe $2p_{3/2}$ can be resolved into two chemical states: Fe^{3+} (710.6 – 710.8eV) and Fe^0 (707eV)
- Fe on the surface is strongly oxidized while as penetration depth increases Fe becomes more reduced
- Predominance of oxidized Fe in MgO/Fe suggest possible reaction
- Inward diffusion of Fe is lowest in Al_2O_3/Fe

Amama, Pint, Mirri, Pasquali, Hauge, Maruyama, *Carbon*, **2012**, *50*, 2396

Summary (II)

- The catalytic activity increases in the following order: **sapphire/Fe < annealed/Fe < ALD/Fe < e-beam/Fe < sputtered/Fe**
- SWCNT carpet growth is maximized by **very low Ostwald ripening rate, mild subsurface diffusion rate, and high porosity,** which is best achieved in sputtered/Fe
- Our results will benefit current efforts aimed at rational design of catalysts with longer lifetime and enhanced activity for SWCNT carpet growth

Outline

- Motivation and overview
- Role of water and growth termination
  - *Ostwald ripening & subsurface diffusion phenomena*
- Influence of support-metal interactions (SMI)
  - *Carpet growth (catalyst activity & lifetime)*
  - *3D evolution of the catalyst*
- Features of a good catalyst support
  - *Porosity*
  - *Active site density*
  - *Powerful tool for predicting activity of supports*
- Conclusions

Surface Roughness and Porosity of Alumina

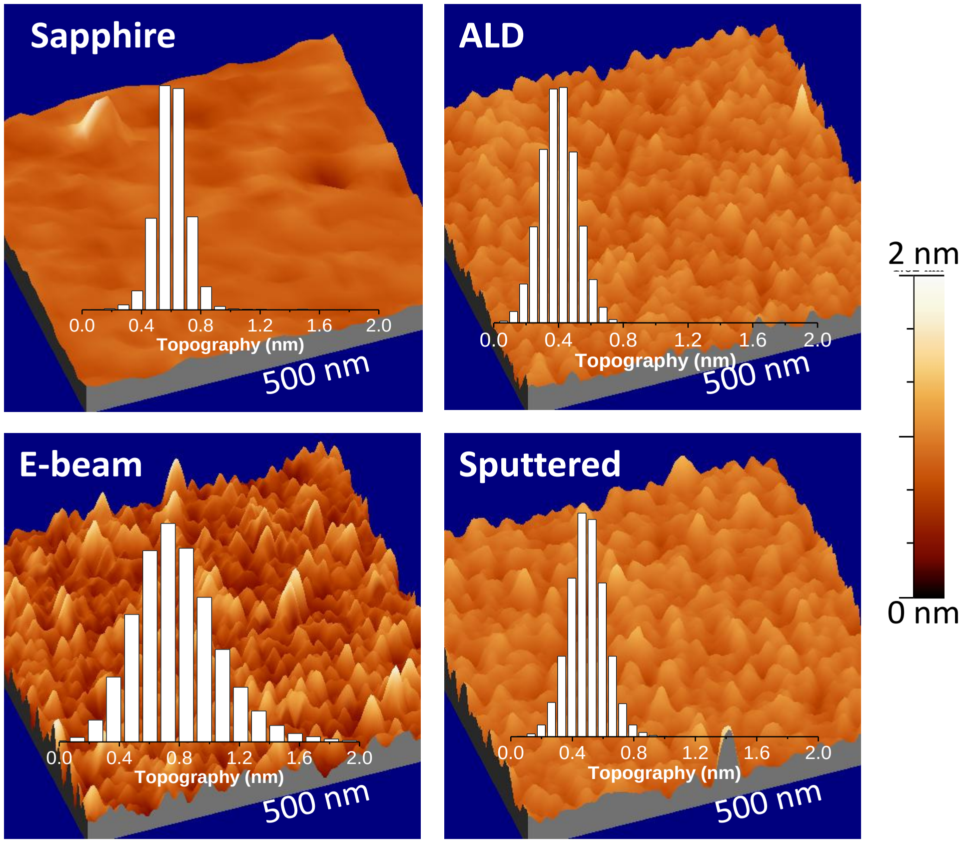

Alumina sample	RMS roughness (nm)	Refractive index (n) at 750nm*
Sapphire	0.10 ± 0.01	1.77
ALD	0.15 ± 0.02	1.63
E-beam	0.27± 0.02	1.57
Sputtered	0.14± 0.01	1.47

*Determined using ellipsometry

- The surface topography and geometry strongly influences the contact angle measurement
- Contact angle measurement is unaffected if R_{rms} is in the subnanometer range; R_{rms} values are in the range of 0.1 – 0.3 nm

Surface Analysis Techniques

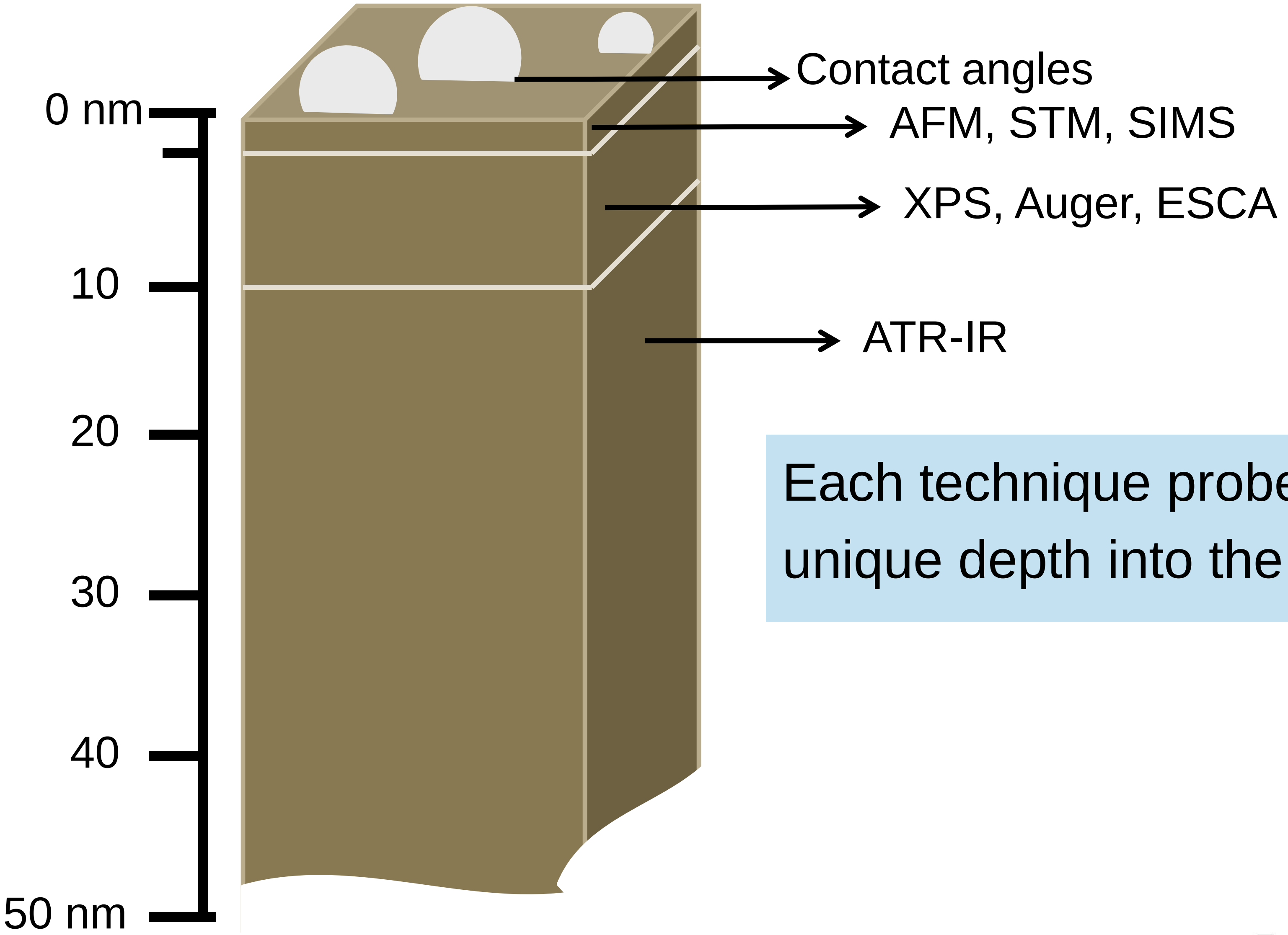

Each technique probes a unique depth into the surface

Surface Energy: Wetting Phenomena

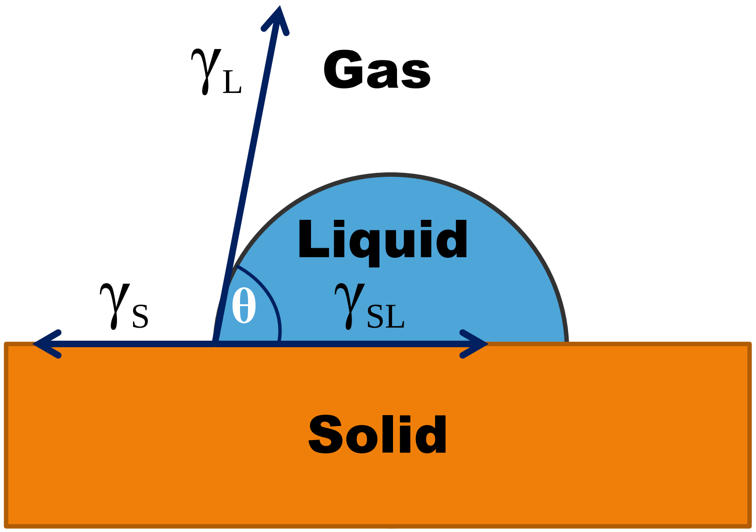

The Young's equation relates the contact angle θ of a sessile drop to the interfacial surface energies:

$$\gamma_S = \gamma_L \cos(\theta) + \gamma_{SL}$$

γ_S: solid-vapor surface energy
γ_L: liquid-vapor surface energy
γ_{SL}: solid-liquid interfacial energy

- θ is a measure of the competing tendencies between the energy of cohesion of the liquid molecules and the energy of adhesion between the solid and liquid

- The higher the water contact angle, the more hydrophobic the solid surface and the lower the surface free energy

- Alumina surface is usually covered with OH groups, which have strong attractive interactions with polar molecules like water.

AFRL

Static Water Contact Angles for Alumina Surfaces

	Sapphire		E-beam		ALD		Sputtered	
Droplets	LCA (°)	RCA (°)	LCA (°)	RCA (°)	LCA (°)	RCA (°)	LCA (°)	RCA (°)
1	69.63	68.28	60.12	59.62	56.14	56.24	54.67	52.35
2	72.55	73.57	62.54	60.53	58.06	57.00	62.91	63.85
3	72.78	70.78	61.36	63.08	57.44	56.93	62.43	63.75
4	71.67	72.14	59.49	59.61	58.47	58.42	63.15	62.34
5	77.53	75.13	65.22	64.54	59.76	59.60	63.03	63.93
6	75.65	75.86	62.32	62.13	58.94	59.32	59.70	61.70
7	74.99	73.84	61.06	61.19	60.73	60.47	63.12	62.60
8	78.80	79.10	62.56	62.38	62.90	62.91	57.13	51.97
9	61.79	67.67	59.86	60.26	62.56	62.29	58.56	55.68
10	71.98	67.29	59.71	60.09	61.53	61.32	58.66	55.40
	72.55 ± 4.24		**61.38 ± 1.67**		**59.55 ± 2.22**		**59.84 ± 4.01**	

Surface free energy: sapphire < amorphous films

Surface Energy Calculations

According to the Oss-Chaudhury-Good (VOCG) model, the total surface energy γ_{TOT} consist of two components:

$$\gamma_{TOT} = \gamma^{LW} + \gamma^{AB}$$

γ^{LW}: apolar component; accounting for Lifshitz-van der Waals interactions

γ^{AB} : polar component; accounting for acid-base or electron donor-acceptor interactions

$$\gamma^{AB} = 2\sqrt{\gamma^{+}\gamma^{-}}$$

γ^{+}: Lewis-acid component, electron acceptor

γ^{-}: Lewis-base component, electron donor

The relationship between γ^{LW}, γ^{+}, and γ^{+} of a solid surface and the known γ_L of probe liquidscan be determined using the Young-Dupré equation:

$$\gamma_L(\cos\theta_L + 1) = 2\left(\underbrace{\sqrt{\gamma_S^{LW}\gamma_L^{LW}}}_{\text{Apolar}} + \underbrace{\sqrt{\gamma_S^{+}\gamma_L^{-}} + \sqrt{\gamma_S^{-}\gamma_L^{+}}}_{\text{Polar}}\right)$$

van Oss et al. *Chem. Rev.* **1988**, *88*, 927

θ as a Force Balance Equilibrium for a Drop of Liquid on a Support

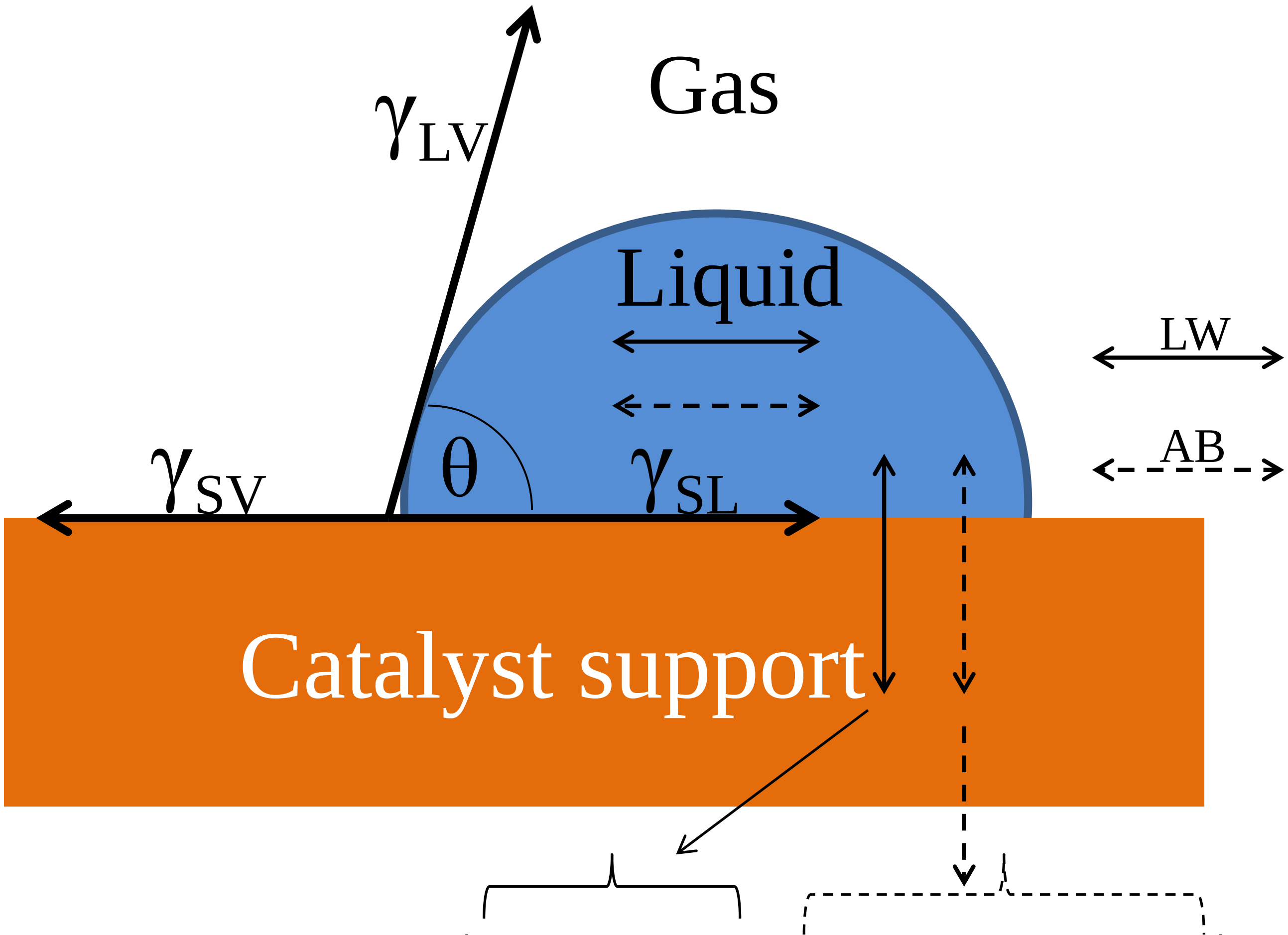

$$\gamma_L(\cos\theta_L + 1) = 2\left(\sqrt{\gamma_S^{LW}\gamma_L^{LW}} + \sqrt{\gamma_S^{+}\gamma_L^{-}} + \sqrt{\gamma_S^{-}\gamma_L^{+}}\right)$$

Surface Free Energy Components

Young Dupré equation: $\gamma_L(\cos\theta_L + 1) = 2\left(\sqrt{\gamma_S^{LW}\gamma_L^{LW}} + \sqrt{\gamma_S^{+}\gamma_L^{-}} + \sqrt{\gamma_S^{-}\gamma_L^{+}}\right)$

Alumina support	**Surface free energy components and total surface free energy (mJ/m^2)**					**Carpet height (μm)**
	Apolar, γ^{LW}	Polar, γ^{AB}	Acidic, γ^{+}	**Basic, γ^{-}**	γ_{TOT}	*After 15 min*
Sapphire	26.7	9.9	2.1	**11.9**	36.7	0
ALD	45.0	7.4	0.2	**56.3**	52.4	12.0
E-beam	39.3	10.1	0.4	**61.9**	49.4	20.0
Sputtered	38.0	7.6	0.2	**65.7**	45.6	29.2

Contact Angle Measurement

Young-Dupré Equation: $\gamma_L(\cos\theta_L + 1) = 2\left(\sqrt{\gamma_S^{LW}\gamma_L^{LW}} + \sqrt{\gamma_S^{+}\gamma_L^{-}} + \sqrt{\gamma_S^{-}\gamma_L^{+}}\right)$

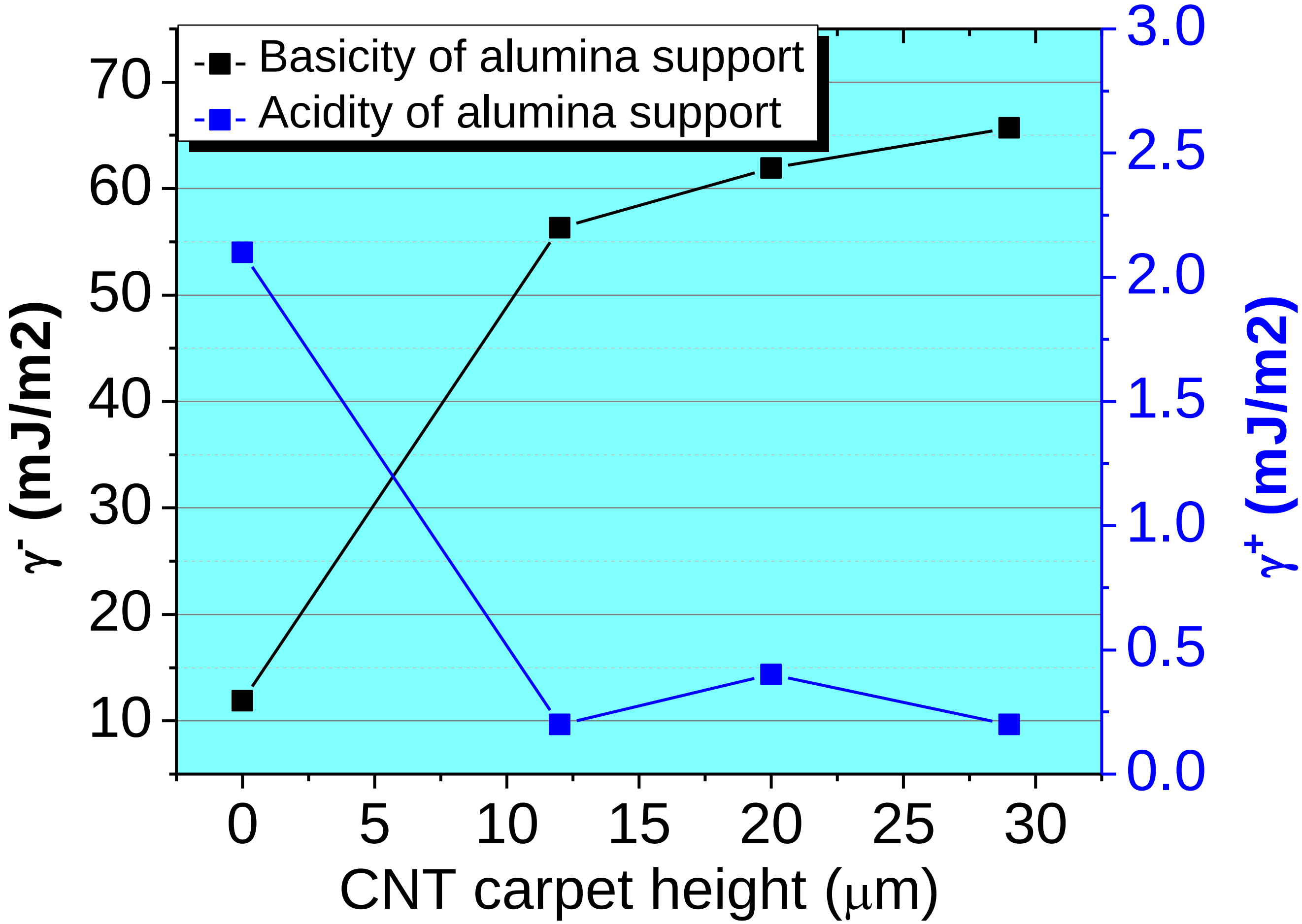

Amama, Putnam, Barron, & Maruyama (Manuscript in review)

Surface Free Energy Components

- The apolar component is the major surface free energy component
- The Lewis basic components (γ^-) are much higher than their Lewis acidic components (γ^+)
- Sputter-deposited alumina shows the strongest basic or electron donating character
  - Magrez et al. (*ACS Nano*, **2011**, *5*, 3428) showed dramatic CNT carpet growth enhancement (1000x longer) when the catalyst support is treated with a basic solution

A simple, reliable, and non-destructive tool based on contact angle measurements is described for predicting the activity of catalyst supports in carbon nanotube (CNT) carpet growth

Amama, Putnam, Barron, & Maruyama (Manuscript in review)

XPS: Hydroxyl Fraction (I)

O ls peak width (FWHM) vs the OH fraction as determined by constrained curve fitting of the peak

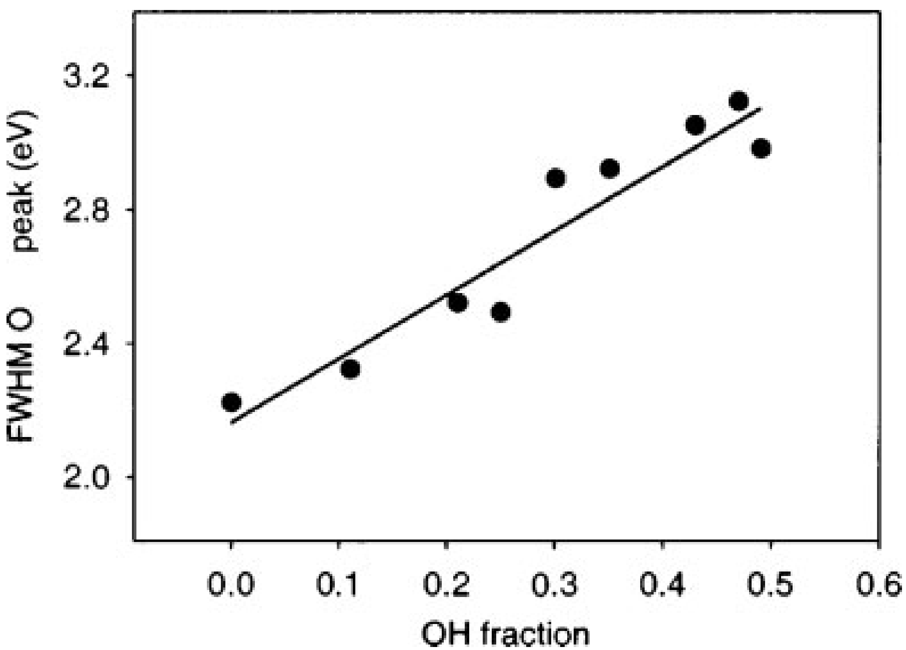

Brand et al. *Surf. Interface Anal.* **2004**, *36*, 81

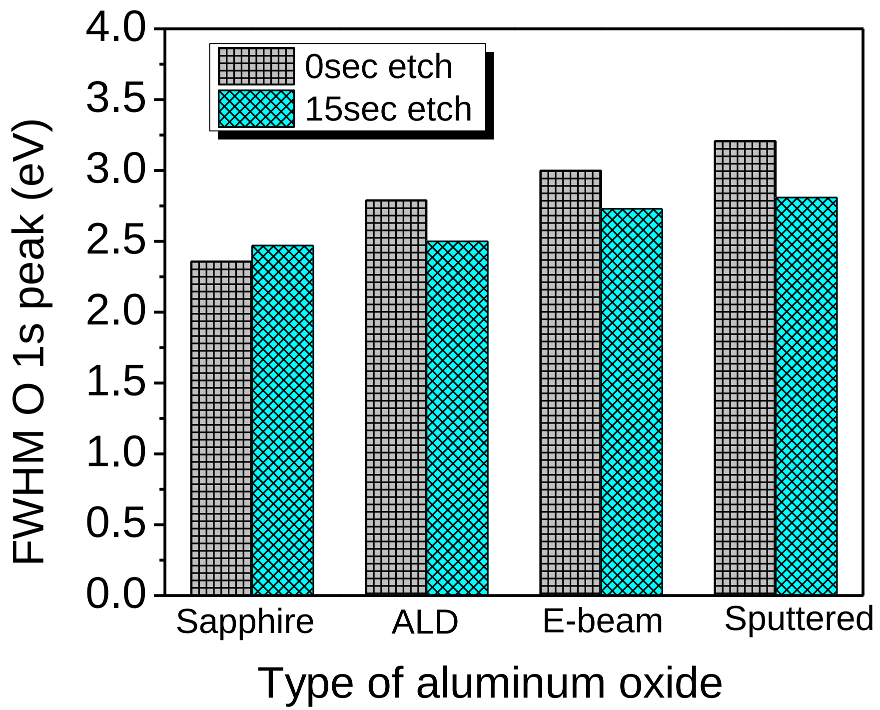

Alumina supports are enriched in hydroxyl groups at the surface/subsurface
Hydroxyl enrichment decreases in the order: Sputtered > e-beam > ALD > sapphire

XPS: Hydroxyl Fraction (II)

Relationship between O/Al atomic ratios and OH fraction

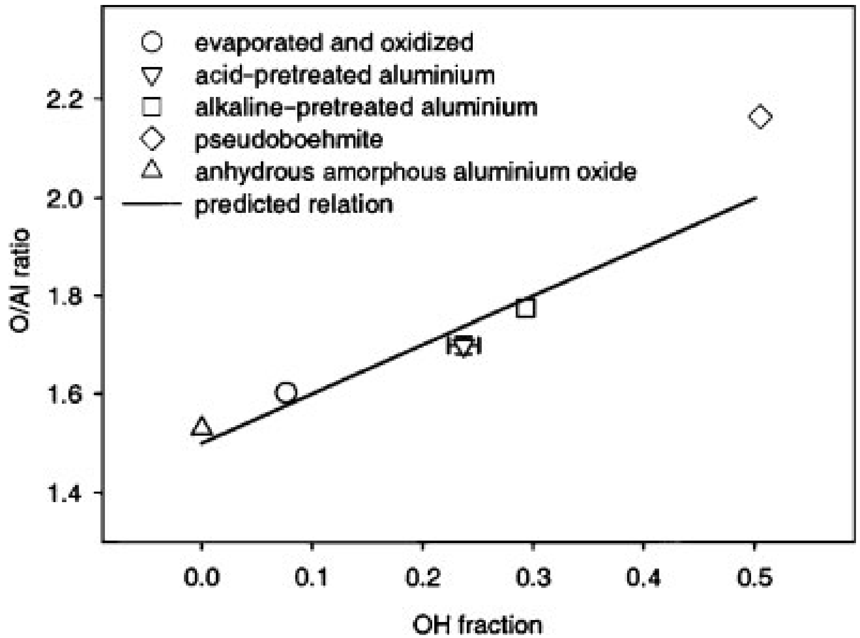

Brand et al. *Surf. Interface Anal.* **2004**, *36*, 81

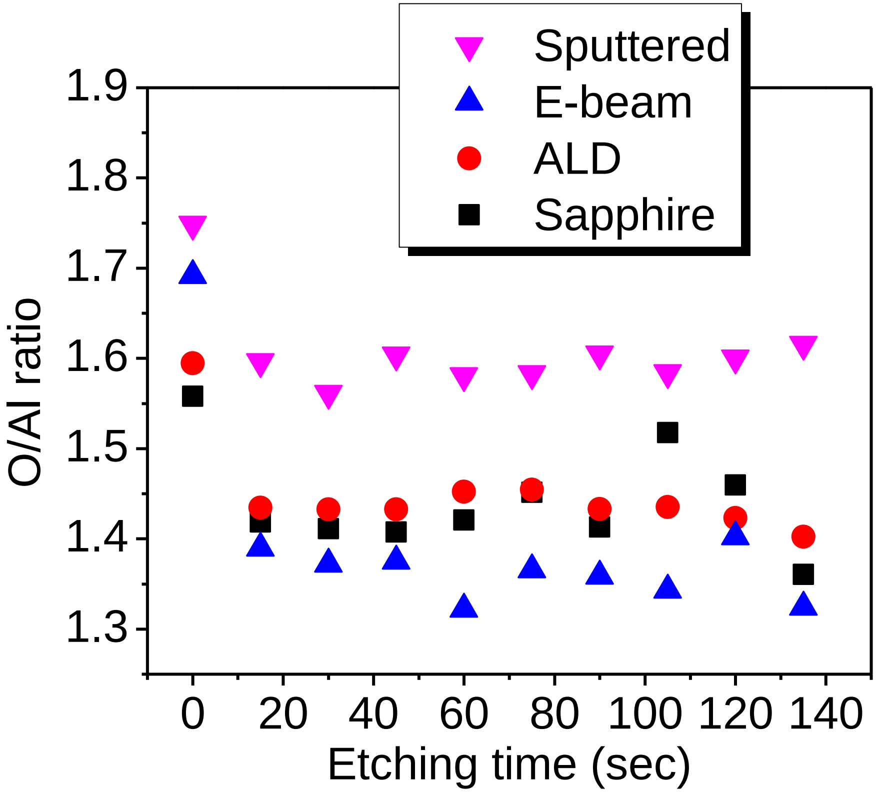

Alumina film thickness: 50nm thick

Alumina supports are enriched in hydroxyl groups at the surface/subsurface
Hydroxyl enrichment decreases in the order: Sputtered > e-beam > ALD > sapphire

Effect of Hydroxyl Enrichment on Carpet Height

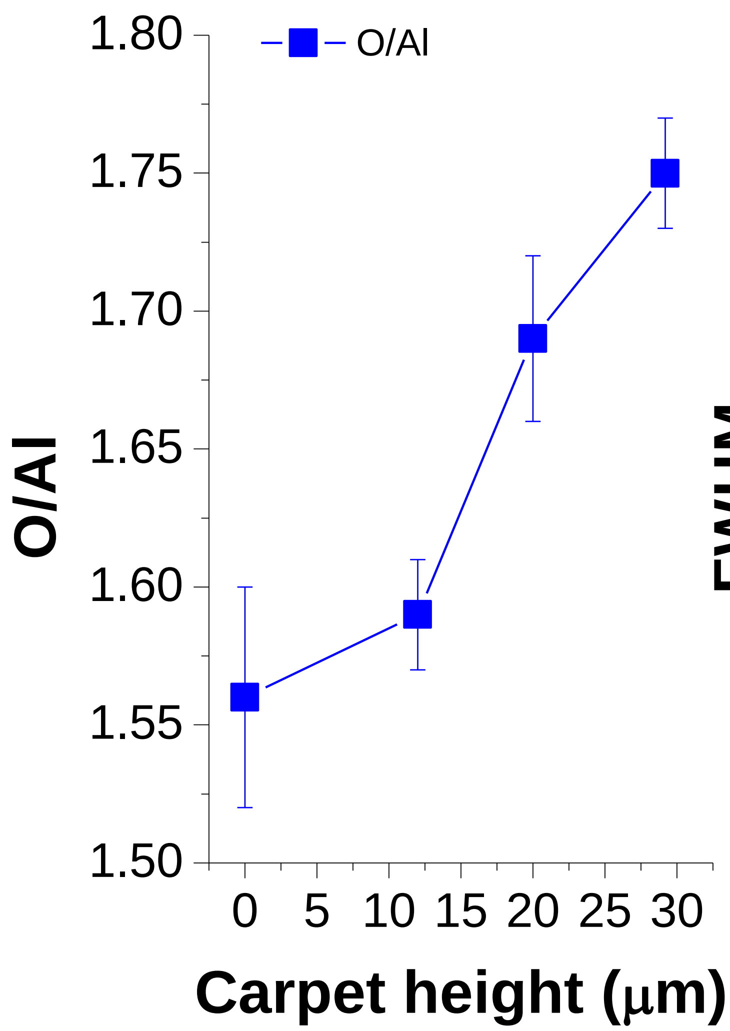

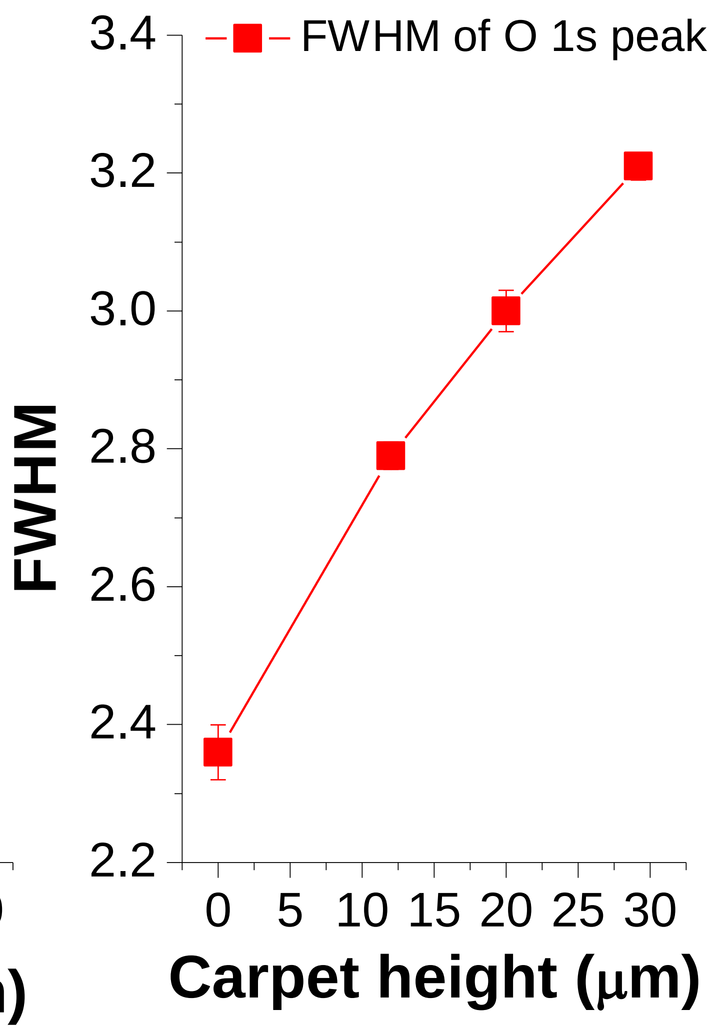

What Makes a Good Support?

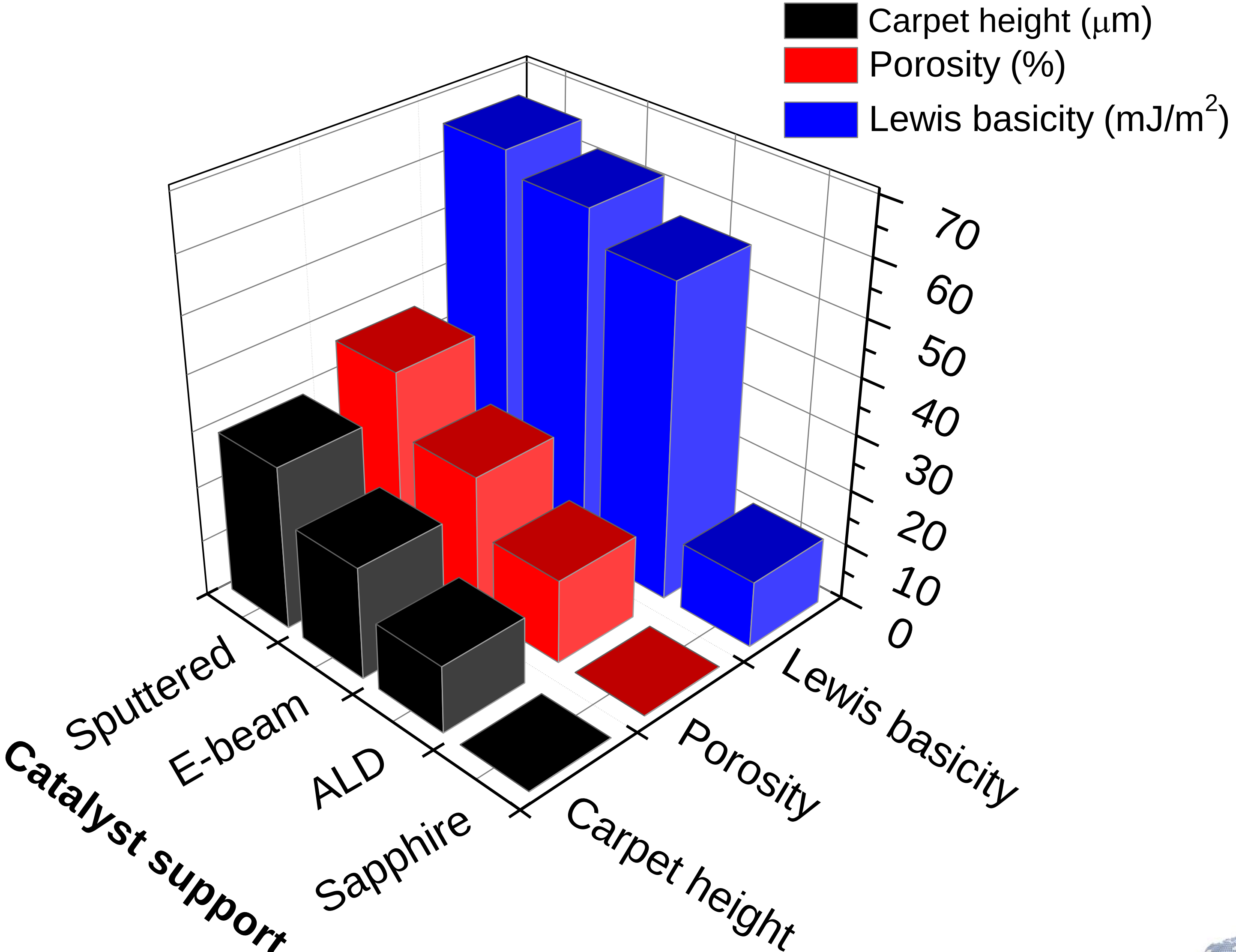

Summary

The catalytic activity of Al_xO_y/Fe during SWCNT carpet growth is enhanced with the following attributes:

- **Support**
  - High porosity of alumina
  - High surface free energy for the Lewis basic component
  - High hydroxyl enrichment on the surface/subsurface
- **Catalyst-support**
  - Low Ostwald ripening rate
  - Mild subsurface diffusion rate

Conclusions

- Dynamic catalyst evolution plays a significant role in growth termination
- SWCNT carpet growth is maximized by very low Ostwald ripening rate, mild subsurface diffusion rate, high porosity, and high surface free energy for the basic component (γ^{-})
- A simple, reliable, and non-destructive tool for predicting the activity of catalyst supports is demonstrated

Acknowledgements

- Air Force Office of Scientific Research (AFOSR)
- Dr. Benji Maruyama (AFRL)
- Dr. Eric Stach (Brookhaven National Lab)
- Dr. Bob Hauge (Rice Univ)
- Prof. Cary Pint (Vanderbilt Univ)
- Dr. Seung Min Kim (Samsung)
- Prof. Shawn Putnam (Univ of Central Florida)

References

(1) Amama, Pint, McJilton, Kim, Stach, Murray, Hauge, Maruyama, *Nano Lett.* **2009**, *9*, 44.

(2) Amama, Pint, Kim, McJilton, Eyink, Stach, Hauge, Maruyama, *ACS Nano* **2010**, *4*, 895.

(3) Kim, Pint, Amama, Zakharov, Hauge, Maruyama, Stach, *J. Phys. Chem. Lett.* **2010**, *1*, 918.

(4) Kim, Pint, Amama, Hauge, Maruyama, Stach, *J. Mater. Res.* **2010**, *25*, 1875.

(5) Amama, Pint, Mirri, Pasquali, Hauge, Maruyama, *Carbon*, **2012**, *50*, 2396

(6) Amama, Putnam, Barron, Maruyama, (Manuscript in review)

Acknowledgements

- Air Force Office of Scientific Research (AFOSR)
- Dr. Benji Maruyama (AFRL)
- Dr. Eric Stach (Brookhaven National Lab)
- Dr. Bob Hauge (Rice Univ)
- Prof. Cary Pint (Vanderbilt Univ)
- Dr. Seung Min Kim (Samsung)
- Prof. Shawn Putnam (Univ of Central Florida)